CR-159741
NAS3-20054

National Aeronautics and
Space Administration

PROGRAM TO DEVELOP SPRAYED, PLASTICALLY DEFORMABLE COMPRESSOR SHROUD SEAL MATERIALS

INTERIM TECHNICAL PROGRESS REPORT NO. 1

JUNE 29, 1976 - FEBRUARY 28, 1979

(NASA-CR-159741) PROGRAM TO DEVELOP N80-16338
SPRAYED, PLASTICALLY DEFORMABLE COMPRESSOR
SHROUD SEAL MATERIALS Interim Technical
Progress Report, 29 Jun. 1976 - 28 Feb. 1979 Unclas
(General Electric Co.) 78 p HC A05/MF A01 G3/37 11944

BY
R.C. SCHWAB
MATERIALS AND PROCESS TECHNOLOGY LABORATORIES
AIRCRAFT ENGINE GROUP
GENERAL ELECTRIC COMPANY
CINCINNATI, OHIO 45215

Prepared for
NATIONAL AERONAUTICS AND SPACE ADMINISTRATION
LEWIS RESEARCH CENTER
21000 BROOKPARK ROAD
CLEVELAND, OHIO 44135

NAS3-20054

National Aeronautics and
Space Administration

PROGRAM TO DEVELOP SPRAYED, PLASTICALLY DEFORMABLE COMPRESSOR SHROUD SEAL MATERIALS

INTERIM TECHNICAL PROGRESS REPORT NO. 1

JUNE 29, 1976 - FEBRUARY 28, 1979

BY
R.C. SCHWAB
MATERIALS AND PROCESS TECHNOLOGY LABORATORIES
AIRCRAFT ENGINE GROUP
GENERAL ELECTRIC COMPANY
CINCINNATI, OHIO 45215

Prepared for
NATIONAL AERONAUTICS AND SPACE ADMINISTRATION
LEWIS RESEARCH CENTER
21000 BROOKPARK ROAD
CLEVELAND, OHIO 44135

1. Report No.	2. Government Accession No.	3. Recipient's Catalog No.
CR159741		

4. Title and Subtitle	5. Report Date
Program to Develop Sprayed, Plastically Deformable Compressor Shroud Seal Material	November 1979
	6. Performing Organization Code
7. Author(s) R. C. Schwab	8. Performing Organization Report No.
	10. Work Unit No.
9. Performing Organization Name and Address Aircraft Engine Group General Electric Company Cincinnati, Ohio 45215	11. Contract or Grant No. NAS3-20054
	13. Type of Report and Period Covered Contractor Report
12. Sponsoring Agency Name and Address National Aeronautics and Space Administrator Washington, D.C. 20546	14. Sponsoring Agency Code

15. Supplementary Notes Interim Report
Project Manager, H. W. Scibbe
Technical Advisor, R. C. Bill
Mechanical Components Branch, Fluid System Components Division
NASA-Lewis Research Center Cleveland, Ohio 44135

16. Abstract

A study of fundamental rub behavior for ten dense sprayed materials and eight current compressor clearance materials has been conducted. A literature survey of a wide variety of metallurgical and thermophysical properties was conducted and correlated to rub behavior. Based on these results, the most promising dense rub materials was Cu-9Al. Additional studies on the effects of porosity, incursion rate, blade solidity and ambient temperature were carried out on aluminum bronze (Cu-9Al-1Fe) with and without a 5 5B Feltmetal underlayer.

17. Key Words (Suggested by Author(s))		18. Distribution Statement
Compressor	Copper based alloys	UNCLASSIFIED - UNLIMITED
Gas Path Seal	Plasma Spray	
Abradability	Titanium blades	
Nickel base alloys	Coatings	
Iron base alloys		

19. Security Classif. (of this report)	20. Security Classif. (of this page)	21. No. of Pages	22. Price*
UNCLASSIFIED	UNCLASSIFIED		

*For sale by the National Technical Information Service, Springfield, Virginia 22161

NASA-C-168 (Rev. 10-75)

FOREWORD

This report describes the results of a study of the fundamental rub behavior of experimental sprayed materials and currently used compressor clearance materials. This investigation was conducted from July 1976 through February 1979. In addition to the author, the following General Electric Company personnel made significant technical contributions to this effort: W. P. Foster and J. P. Young in conducting the seal rub tests, and Dr. I. I. Bessen for his technical guidance in analysis of the data. Dr. S. O. Brennom, while an employee of General Electric Company (currently with Union Carbide Corporation in Indianapolis, Indiana), contributed significantly to the overall effort.

TABLE OF CONTENTS

LIST OF FIGURES

LIST OF FIGURES
(continued)

LIST OF TABLES

1.0 SUMMARY

Ten metals were selected for the Task I - Phase I study of fundamental rub behavior of materials by titanium compressor blade. A wide range of metallurgical characteristics (crystal structure, density, composition, mechanical properties)and thermo-physical properties (melting point, specific heat, thermal conductivity, and thermal expansion coefficient) were covered by the materials selected. These were Al, Fe, Cu, Zn, Cu-10Zn, Cu-5Al, Cu-9Al, Fe-6Al, Fe-13Cr, and Ni-13 Cr. Such properties as impact strength, thermal conductivity, and melting point appear to play significant roles in rub behavior, but do not completely account for the differences observed in the rub behavior of these materials.

A number of current compressor clearance control coatings were investigated in Task I, Phase II. These included Al, Metco 601, AlBronze/NiCg, 80/20 NiCg, AB-1, Feltmetal 515B, Al top coat over Feltmetal, and Albronze top coat over Feltmetal. Results for the aluminum were in reasonable agreement with the data from Phase I. The only materials which caused blade wear were the Albronze/NiCg and the 80/20 NiCg. On the basis of both Phases I and II it was found that rub energy cannot be used as a screening test for compressor clearance control coating materials.

As a result of Phases I and II, Cu-9Al was identified as the most promising clearance control coating material. In Task I, Phase III Cu-9Al was studied at two porosity levels (with 20 & 40% Ekonol added) with a Feltmetal 515 B underlayer and without the FM 515 B underlayer. The 20% porosity material exhibited good rub characteristics both with and without the Feltmetal 515 B underlayer for the Cu-9Al since it was expected to give similar rub behavior (composition = Cu-9.5 Al-1Fe) and was more readily available than the Cu9Al. Rub tests were conducted at 0.0001 and 0.001 inch/sec incursion rates at room temperature and 900°F with 48 blades and 12 blades. It was found that for the low incursion rate, hot rubs were more severe than cold rubs, but at the higher incursion rate cold rubs were more severe than hot rubs. The presence of the Feltmetal 515B was beneficial in reducing blade wear.

2.0 RECOMMENDATIONS

1) Work is needed to identify the reason why Al additions to Cu improves rub behavior. Areas that warrant further investigation include: a) the possibility that Al reduces the tendency of Cu-Ti eutectic formation; b) the effect of Al on the melting point/thermal conductivity of the alloys; and c) the possible role of impact properties on rub behavior since the high rub velocities approach impact conditions.

2) A better definition of the powder requirements and spray process parameters is needed as subtle changes were found to affect rub behavior.

3) Both the AlBr/20% Ekonol and AlBr/20% Ekonol over Feltmetal coatings have demonstrated acceptable abradability, blade wear and smooth rub requirements. The next step should be to determine and/or demonstrate the erosion, thermal shock and oxidation resistance of the coatings.

3.0 INTRODUCTION

A major factor in the progress of aircraft engine development has been continued improvement in engine performance. In turn, many performance improvements have been dependent upon advancements in materials and process technology. Improved compressor clearance control has contributed to performance improvement through the application of abradable gas path seal materials. These materials have included thermal-sprayed aluminum and nickel graphites, Feltmetals, and silicone rubbers.

Compressors for advance turbine engines are designed with higher pressure ratios, fewer stages (higher loading per stage), and higher tip speeds than prevail in current production engines. Under these conditions, leakage over compressor blade tips results in substantial performance losses. Efforts to reduce those losses by decreasing tip clearances are frequently thwarted by excessive tip rubs caused by such events as transient compressor stalls, gyroscopic flight loads, and engine inlet distortion. These rubs lead to: 1) blade wear and consequent increased clearance; 2) blade tip fatigue failures caused by excitation from rubbing; and 3) generation of particulate debris which clogs air passages in downstream cooled turbine hardware, sticks to blades, and decreases performance; 4) and sometimes thermal damage to Ti-alloy rotor and stator components. Rub coatings or rub materials that are: 1) abradable under high speed rubs and produce minimal damage to blade tips; 2) that retain tight clearances; and 3) that generate a nonsticking, nonreacting rub debris, will produce significant performance improvements in both current production and future engines.

Clearance control seal materials have assisted engine designers in improving the compressor efficiency of aircraft gas turbine engines. However, current materials are not adequate for advanced engines, being deficient from blade wear, erosion resistance, debris character and/or surface finish aspects. Plasma sprayed aluminum used on some engines can wear blades or can be scoured depending on engine conditions. Flame sprayed nickel graphite coatings used in other engines can wear blades or erode excessively depending on the composition and strength level of the coating, and good surface finishes are difficult to obtain.

All of the materials that rub well, i.e., that produce little or no blade wear, display either of two characteristics: 1) they have low cohesive strength; or 2) they are easily, plastically deformed. The low cohesive strength materials wear by internal fractures under the blade rub; the plastically deformed materials visually and microscopically look smeared. On so called "hot rubs", the blade tips are worn and show similar plastic flow. Both fracture stress and flow stress are temperature dependent, and therefore, the wear phenomena are intricately dependent on the generation of heat during a rub and the rate of heat loss from the rubbing interfaces.

The low cohesive strength materials have two inherent deficiencies, low erosion resistance and lack of good surface capability. To date most

dense materials have caused blade wear, blade tip fatigue cracking, and/or sticky debris, but they have inherently good surface finish and erosion properties and offer great potential for improved compressor shroud seal performance if their deficiencies can be eliminated. A basic understanding of the deformation processes occurring at the rub surfaces is needed in order to effectively identify solutions to blade wear and fatigue associated problems with dense rub materials. This is especially true with Ti-base blades.

The objectives of this program were: 1) to observe the rub behavior with titanium blades of dense sprayed materials and determine their significant mechanical and physical properties; 2) to select those dense materials on the basis of the deduced properties and subject them to a series of tests designed to meet compressor clearance rub materials requirements and; 3) to assess the effects of adding porosity to these materials.

The program was divided into two tasks. Task I consisted of three phases. In Phase I, ten materials displaying a range of metallurgical properties were selected to evaluate the hot and cold rub test behavior of the dense sprayed coatings in order to determine the properties significant to rub behavior. Current engine compressor seal coatings were evaluated in Phase II and compared to the results of Phase I. Two experimental coating systems were selected based on the results of Phases I and II for use in Phase III where the effect of porosity on the coating rub behavior was examined.

For Task II, two coating systems were selected from Task I results. Further performance verification of the two systems was undertaken, consideration being given to a wide range of rub test parameters, and such aspect of performance as thermal shock resistance effect of long term temperature and erosion resistance.

4.0 TEST PROGRAM

The test program was designed to identify a material system(s) as a potential improved compressor clearance coating from a study of the rub behavior of a variety of dense sprayed materials and current engine compressor coatings. A flow chart for the test program is given in Figure 1.

TEST PROGRAM FLOW DIAGRAM

a) TASK I

PHASE I - FULLY DENSE MATERIAL DEVELOPMENT

MATERIALS SELECTION (10)

Material	Melting Pt	Structure
Al	1215F	FCC
Cu	1980F	FCC
Cu-5Al	1940F	FCC
Cu-9Al	1908F	FCC
Cu-10Zn	1910F	FCC
Ni-13Cr	2606F	FCC
Zn	727F	HCP
Fe	2795F	BCC
Fe-6Al	2785F	BCC
Fe-13Cr-.1Cb	2770F	BCC

↓

MATERIAL FABRICATION

TEN THERMAL SPRAY LOTS - ONE SPRAY EACH

↓

RUB TESTING

TWO RUBS/MATERIAL - ONE COLD, ONE HOT

↓

MATERIAL CHARACTERIZATION

Computer Literature Search - 10 Materials

- Chemical Properties
- Metallurgical Properties
- Crystallographic Properties

↓

DEDUCTION OF SIGNIFICANT CHEMICAL METALLURGICAL AND CRYSTALLOGRAPHIC FEATURES

Figure 1.

TASK I

PHASE II - TESTING OF CURRENTLY USED RUB COATINGS

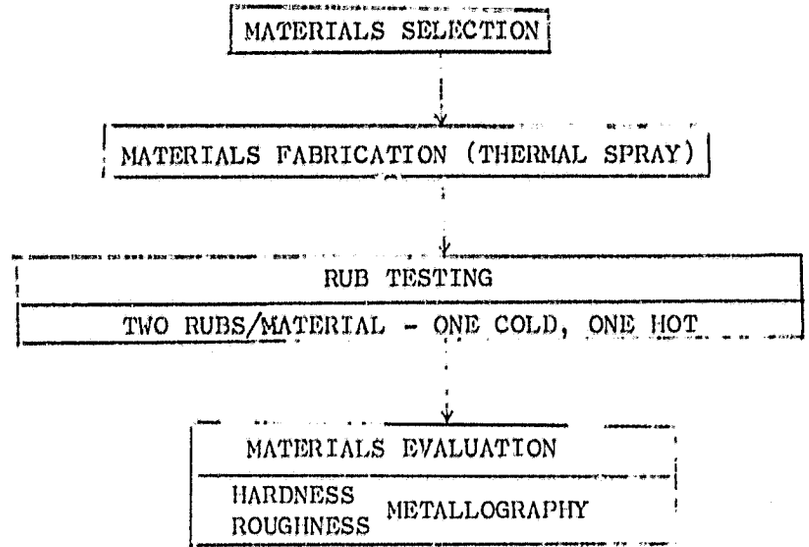

TASK I

PHASE III - MIXED EASY SHEAR POROUS MATERIALS

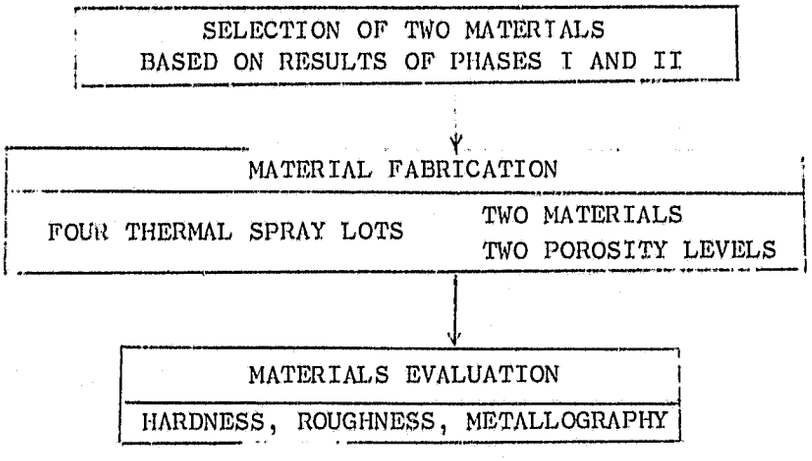

b) TASK II

RUB TEST PARAMETER EVALUATION

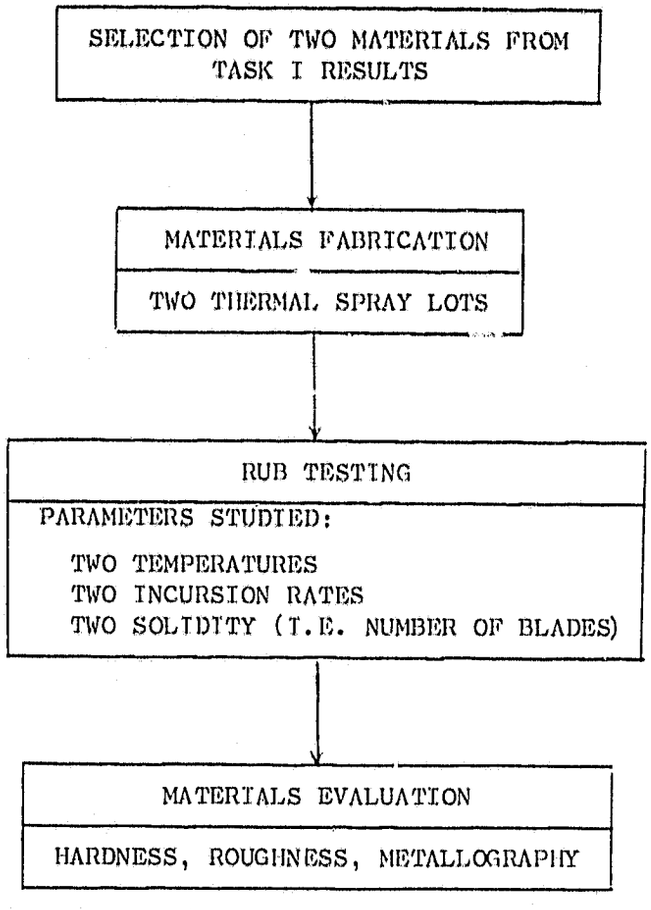

4.1 Test Procedures

The rub tester used consisted of a steam driven rotating blade fixture (Figure 2) capable of holding up to 48 blades and producing a maximum blade speed of 500 fps. The blade axis is parallel to the rotation axis. The shroud material is located on a static specimen (Figure 3) with its rub face in a plane perpendicular to the rotating axis or (intentionally) tilted at a small angle. The rub is made by translating the static member into the rotating blade tips. The ambient temperature of the rig can be set as high as 1200°F with a drift in temperature of less than 20°F. A dynanometer stage mounted on the stator is capable of measuring shear forces as low as 0.5 lb. The specimen substrate temperature and the rub force (dynamometer) were continuously monitored during the rub tests and recorded on a strip chart (Figure 4).

A cold particle erosion test was also employed in which 50μ Al_2O_3 particles are jetted through a standard nozzle at 40 psi air pressure with a 20° impingement angle on a 1" x 2" specimen set at 4" from the nozzle. Like most particle erosion tests, it provides a bench mark of material density, cohesive strength, and hardness by measuring pit depth in a standard length of time from which an erosivity number (seconds to erode 1 mil can be calculated. Usually the more resistant materials, being dense are less permeable to gas penetration and more resistant to gas erosion as well.

4.2 Task I

4.2.1 Phase I - Significant Property Identification

4.2.1.1 Material Selection and Preparation

The basic explanation of what occurs when a blade rubs into a seal is that the stronger material will resist wear and the weaker material will take the wear. If one material has a low fracture strength, it will break away in pieces in preference to the material with high fracture strength. Similarly, if one material has an easy tendency to flow plastically (i.e., a low flow stress), it will wear by smearing in preference to the other which may not deform plastically at all. Complexities arise when one considers the effect of fracture stress and flow stress due to changes in temperature of the rubbing members. There is never a certainty that both rubbing members will exist at the same temperature during a rub. Although all blade materials have high fracture strengths, they do not always have high flow stresses. Titanium alloys, in particular, lose strength rapidly with increasing temperature, and plastic flow sets in across Ti blade tips quite readily to produce burrs when the tip is overheated. Titanium blades that have been severely worn also have shown a blue oxide across the tip, indicating that excessive temperatures have been attained due to the energy dissipated during the rub.

Blade rubbing requires dynamic consideration. Due to the heat generated at the blade tips during rubbing there are probably competitive

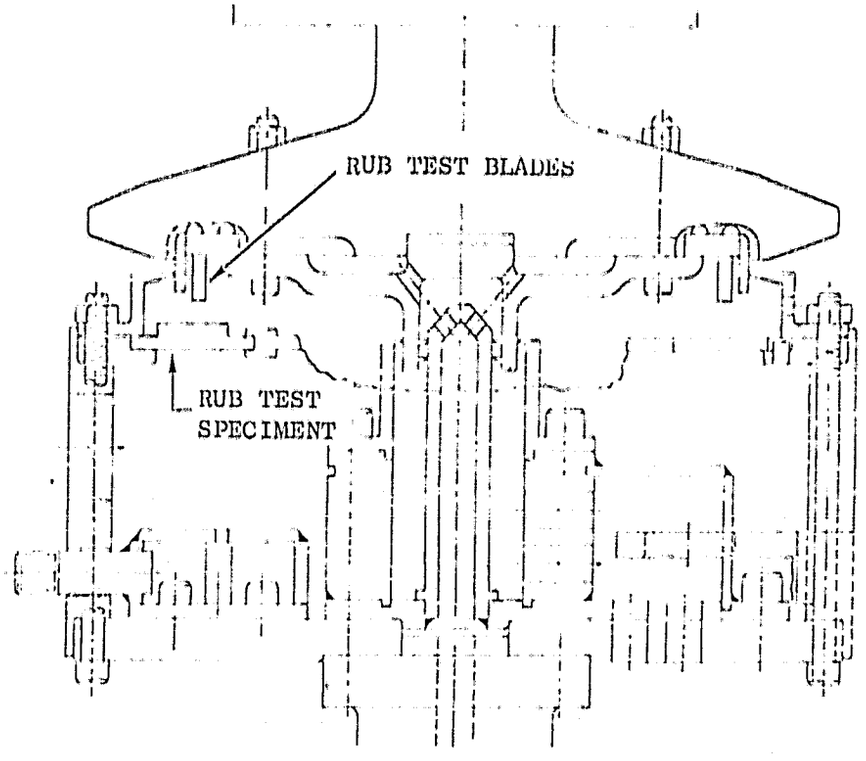

Figure 2. Schematic of the rub test rig showing blades and stator configuration

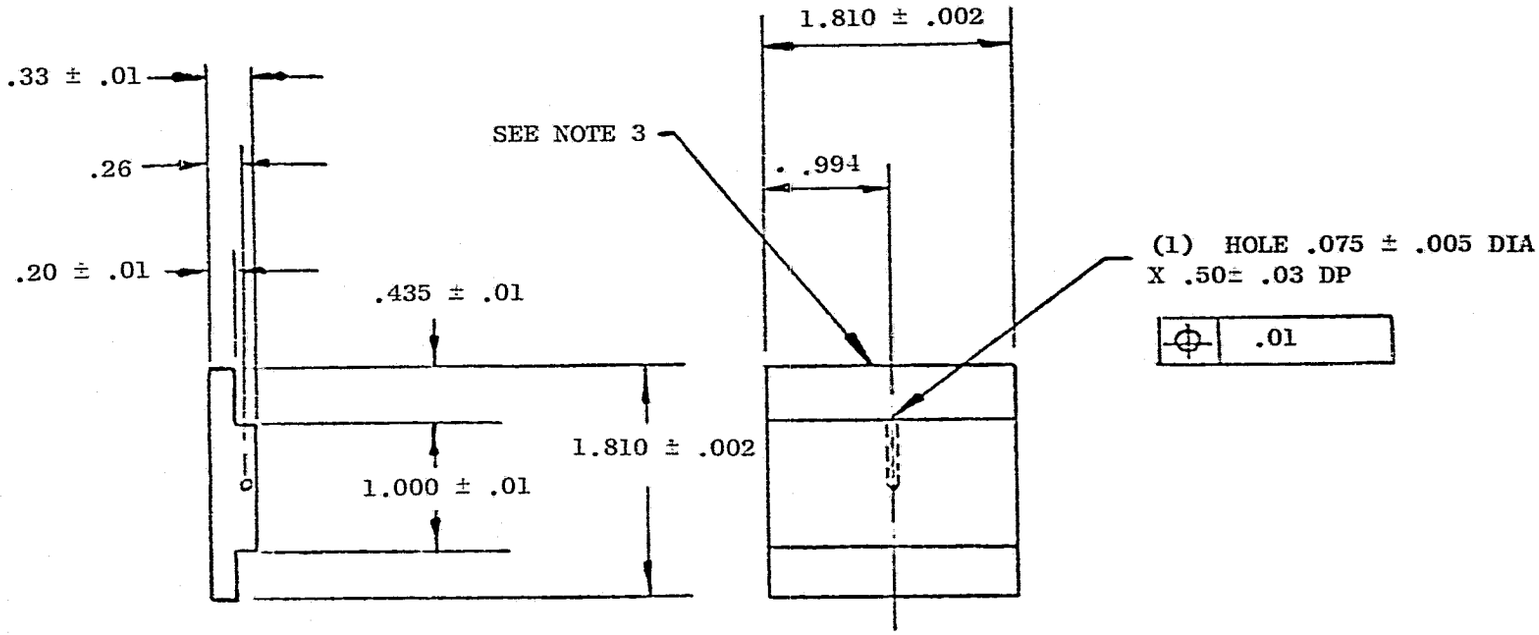

Figure 3. Rub Test Speciments

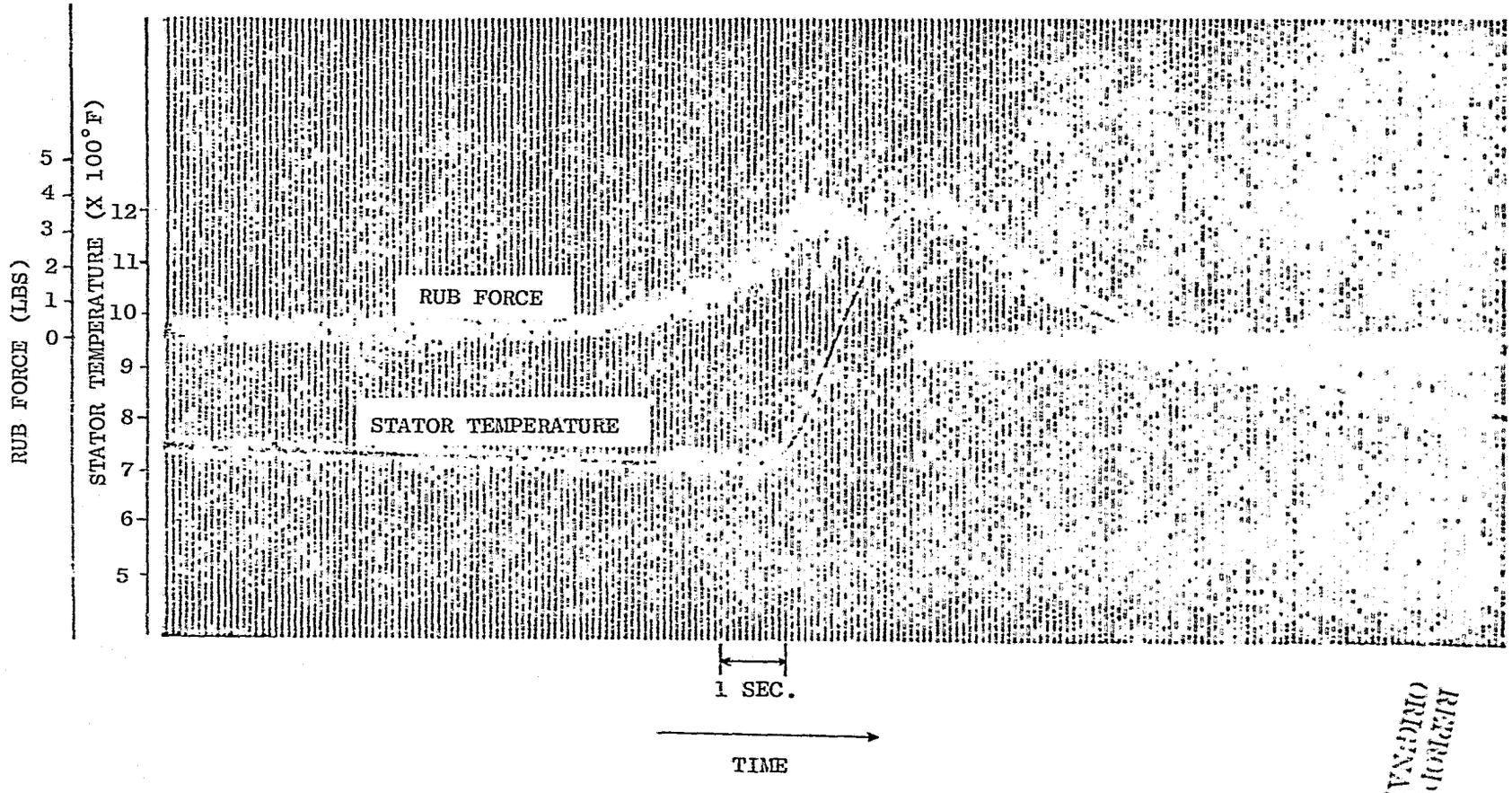

Figure 4. Strip chart trace of test specimen temperature and rub force versus time during the test

reactions such as work hardening versus recrystallization. However, in the Lynn rub tester at blade tip speeds of 500 surface feet per second, a rub occurs every 2 milliseconds and recrystallization will not be kinetically favored unless the temperature is high enough for rapid lattice diffusion. Recrystallization may occur during high speed rubs in alloys with relatively low melting points.

Work hardening will depend upon solute effects (lattice atomic size mismatch) and crystalline structure (number and efficiency of slip planes, cross-slip tendency, and stacking fault energy). These parameters can be explored by varying alloy compositions while maintaining the same crystal structure, and by studying materials with different crystal structures.

Considering the facts above, the following ten materials were selected:

1) Al (FCC) - aluminum is known to display easy shear when rubbed. It is a good reference material with a flow stress lower than Ti alloys.

2) Cu (FCC) - copper provides higher working temperatures than aluminum although it will work harden more due to lower stacking fault energy. Copper also provides a reference material for Cu-Al alloys.

3) Cu-5Al (FCC) - aluminum addition adds oxidation resistance to copper, but it also reduces the stacking fault energy (may increase work hardening).

4) Cu-9Al (FCC) - this alloy when sprayed as a mixture with nickel graphite has shown good engine rub behavior with Ti-base blades. Its stacking fault energy is lower than Cu-5Al.

5) Cu-10Zn (FCC) -Zinc has a small mismatch effect on copper and should give additional information on alloying effects.

6) Ni-13Cr (FCC) - Ni-20Cr has been shown to wear Ti base blades. The flow stress will be lowered by dropping the chromium content.

7) Zn (HCP)-Zinc is known to rub well and should be a good reference material for ideal rub behavior even though its low melting point makes it impractical for engine use.

8) Fe (BCC) - BCC crystals have more slip systems than FCC or HCP crystals, and iron which is low in interstitial carbon and nitrogen will have a relatively low flow stress even though its temperature capability is higher than the copper and aluminum alloys.

9) Fe-6Al (BCC) - aluminum addition will add oxidation resistance to the iron while maintaining BCC structure.

10) Fe-13Cr-0.1Cb (BCC) - chromium addition will add more oxidation resistance to the iron and columbium will minimize cabide and nitride solute hardening by forming columbium carbide and nitride precipitates.

Selected bulk properties from the literature of the ten coating materials are compiled in Table 1.

The surfaces of all rub test panels were grit blasted and thermally sprayed with a 4-8 mil bond coat of Metco 450 (nickel aluminide) to promote good adhesion of the 0.050-0.060" thick top coating. The as-sprayed coating densities were determined by water immersion (Table 2). The low densities of the Fe-base alloys were due to porosity caused by incomplete particle melting during spraying. All coated panels were annealed prior to rub testing.

4.2.1.2 Dense Coating Rub Test Results

The rub parameters used for all the tests were:

Blade material:	Ti-6Al-4V
Number of blades:	48
Blade thickness:	0.025 inch
Incursion rate:	0.010 inch/sec
Incursion depth:	0.020-0.030 inch
Blade tip speed:	500 SFS
Ambient temperature:	100 and 900^{o}F

The rub test results are tabulated in Table 3. Definitions of the columns of the table which are not self-explanatory are as follows:

T_m	Melting point of the coating
$T_{ambient}$	Temperature measured by the control thermocouple at the initiation of a test; the control TC being embedded in the substrate 0.060 inch below the rub coating
T_{max}	The maximum temperature observed by the control TC during a test
Max. temp. rise rate	The maximum slope of the temperature-time trace of the control TC output during a test
Max. shear force	Highest shear force recorded during a test, usually occurring as a peak at the beginning of the test
Min. shear force	The lowest shear force recorded after the peak force was attained

TABLE I

BULK PROPERTIES OF PHASE I COATING MATERIALS

(Room temperature values unless otherwise stated)

Property	Al	Cu	Fe	Zn	Cu-10Zn	Cu-5Al	Cu-9Al	Fe-6Al	Fe-13Cr	Ni-13Cr	Reference
Atomic Composition-%	-	-	-	-	9.7Zn	11.0Al	18.9Al	11.7Al	13.8Cr	14.4Cr	1
Crystal Structure	FCC	FCC	BCC	HCP	FCC	FCC	FCC	BCC	BCC	FCC	2
Lattice Constant (A) a	4.049	3.615	2.866	2.665	3.635	3.641	3.664	2.883	2.871	3.543	2
c	-	-	-	4.947	-	-	-	-	-	-	
Melting Point-°F	1220	1983	2795	786	1910	1940	1908	2785	2770	2606	3
Density (gm/cc)	2.70	8.96	7.87	7.13	8.80	8.17	7.58	7.28*	7.77*	8.62*	4
Specific Heat (cal/gm/°C)	0.215	0.092	0.110	0.092	0.090	0.099+	0.104	0.114‡	0.11+	0.104	4,5
Thermal Conductivity (cal/cm²/cm/°C/sec)	0.57	0.941	0.178	0.27	0.45	0.198	0.144	0.072	0.054+	0.138+	4,6
Thermal Expansion Coeff (10^{-6}cm/cm/°C)	23.6	16.5	11.7	39.7	18.4	16.5	16.5	13.1	9.9+	13.5+	4,7
Young's Modulus (10^6 psi)	9	16	28.5	13.4	17	17	17	29	29	31	4,8,9
Shear Modulus (10^6 psi)	3.4	6	11.6	5.4	6.4	6.4	6.4	11	11	11.7	Calc from 10
Tensile Strength (Annealed Condition) (10^3 psi)	6.8	32	35	2.8	38	65	65	73.7	74	78	4,11,12,13
Yield Strength (Annealed Condition) (10^3 psi)	1.7	10	15	0.35	12	25	25	59.7	44	40	4,11,12,13
Elongation (%) (Annealed Condition)	35	45	40	-	50	55	40	25	25	30	4,11,12,13
Hardness (MN/M^2) Annealed	196	539	686	294	480	843	990	-	1410	1590	4,14
Hard	343	1225	1960	343	1400	1960	1960	3240	3920	2380	
Hot Working Range (°F)	500/950	1400/1600	-	-	1400/1600	1500/1600	1470/1695	2200	2200	2200	4,5,15,16
Recrystallization Temp (°F)	550/600	570	395/575	50	700	660	1100	1100	-	-	4,12,17
Stacking Fault Energy (ergs/cm²)	200/238	40/70	-	-	36	4	2	-	-	-	11,18,19
Izod Impact Strength (Ft/Lbs)		30/40	-	-	30	-	10/15	-	-	-	

*Calc from lattice constants

+Estimated from 4,

‡Estimated from rule of Dulong and Petit

TABLE 2

DENSITIES OF THE SPRAYED COATINGS

Material	Spray Technique	As-Sprayed Density (% Theoretical)
Al	Wire	90
Cu	Wire	86
Fe	Wire	80
Zn	Wire	90
Cu-10Zn	Wire	86
Cu-5Al	Plasma*	86
Cu-9Al	Plasma*	86
Fe-6Al	Plasma*	73
Fe-13Cr-0.1Cb	Plasma*	80
Ni-13Cr	Plasma*	82

*Powder size (-140 + 325 mesh)

TABLE 3

PHASE I RUB TEST DATA

Coating	T_m (°F)	$T_{Ambient}$ (°F)	T_{max} (°F)	$\Delta T = T_{max} - T_{Ambient}$ (°F)	T_{max}/T_m (°R/°R)	Max. Temp. Rise Rate (°F/Sec)	Max. Temp. Rise Rate (°F/Sec)	Shear Force Min. (Lb.)	Shear Force Max. (lb.)	Max. Force Rise Rate (lb./Sec)	Average Blade Wear (inch)	Avg. Depth of Rub (inch)
Zn	727	100	260	160	0.61	93	93	–	< 0.5	–	< 0.001	-0.010
Al	1215	75	640	565	0.66	–	–	1.6	2.3	1.4	< 0.001	-0.016
Al	1215	855	855	0	0.78	0	0	–	1.5	0.16	< 0.001	-0.031
Cu*	1980	110	680	570	0.47	210	210	3.7	5.0	3.5	0.038	0.006
Cu*	1980	790	1035	245	0.61	96	96	0.4	0.96	0.92	0.026	0.007
Fe*	2795	130	230	100	0.21	18.5	18.5	1.1	2.1	3.2	0.020	0.003
Fe	2795	920	1240	320	0.52	112	112	–	0.13	0.04	0.025	-0.008
Cu-5Al	1940	110	1410	1300	0.78	270	270	4.1	7.2	14.4	0.047	0.017
Cu-5Al	1940	920	1150	230	0.67	90.5	90.5	1.1	1.4	2.4	0.022	-0.016
Cu-9Al	1908	110	1340	1230	0.76	260	260	3.9	7.6	7.8	0.026	0.005 to -0.020
Cu-9Al	1908	810	1380	570	0.78	150	150	2.1	3.3	5.3	0.014	-0.028
Cu-10Zn*	1910	140	360	220	0.34	88.5	88.5	3.2	5.1	7.8	0.022	0.008
Cu-10Zn*	1910	880	1225	345	0.71	138	138	–	0.64	0.4	0.026	0
Fe-6Al*	2785	130	530	400	0.30	162	162	–	4.8	4.8	0.018	-0.007
Fe-6Al*	2785	930	1185	255	0.51	180	180	–	0.58	0.015	0.011	-0.007
Fe-13Cr*	2770	130	500	370	0.30	172	172	–	2.8	3.7	0.019	-0.005
Fe-13Cr*	2770	1000	1290	290	0.54	141	141	–	0.5	0.36	0.019	-0.008
Ni-13Cr*	2606	120	195	75	0.21	13	13	–	2.4	2.3	0.015	(Coating delaminat
Ni-13Cr*	2606	835	955	120	0.46	28.5	28.5	–	1.3	0.49	0.013	0.007

Coating Hardness R_{15Y}	Rub Surface Roughness RMS (Micro-inch)	Rub Surface Appearance	Rub Energy Ft. Lbs. (Btu)	Rub Energy Unit Volum of Coating Removed (ft. lbs. in^3)
84	40-45	Smooth	–	–
89	50-60	Smooth	2730 (3.49)	1.52×10^5
–	–	Smooth	714 (0.914)	4.46×10^4
88	>300	Heavily scabbed	8675 (11.1)	–
85	130	Heavily scabbed	1030 (1.32)	–
94	50	Lightly scabbed	1525 (1.95)	–
94	>300	Lightly scabbed	104 (0.133)	2.60×10^4
91	>300	Heavily scabbed	7702 (9.85)	–
91	>300	Moderately scabbed	1625 (2.08)	2.03×10^5
94	>300	Moderately grooved & scabbed	7780 (9.96)	7.76×10^4
81	75	Lightly grooved & scabbed	5340 (6.83)	3.81×10^4
93	65	Heavily scabbed	1718 (2.2)	–
82	120	Heavily scabbed	864 (1.10)	–
90	>300	Lightly scabbed	2711 (3.47)	7.72×10^5
82	80	Lightly scabbed	471 (0.603)	1.34×10^5
–	–	Lightly scabbed	2065 (2.64)	8.28×10^5
92	80-90	Lightly scabbed	331 (0.425)	8.28×10^4
–	–	Lightly scabbed	2142 (2.74)	–
–	120	Lightly scabbed	1446 (1.85)	–

* Blade contacted only part of specimen surface

Blade material:	Ti-6Al-4V
Number of blades:	48
Blade thickness:	0.025 inch
Incursion rate:	0.010 inch sec
Incursion depth:	0.020-0.030
Blade tip speed:	500 FPS

Max. force rise rate	The maximum slope of the force-time trace recorded during a test
Rub energy	The area under the force-time curve of a test multiplied by the velocity of the blades
Avg. blade wear	Average length change of three randomly selected blades as a result of a rub

Examination of the test results revealed the following trends:

- All of the [illegible] coatings with melting points greater than Al produced blade wear.

- Cu-base alloys caused more severe scabbing and blade wear than Fe or Ni-base alloys during room temperature tests. During elevated temperature rubs, Cu-base alloys with Al additions showed a marked improvement in rub behavior. Cu-9Al coating was the most abradable (most coating wear) of all the materials with melting points greater than aluminum.

- For a given material, elevated temperature rubs exhibited shear forces (rub energy) which were lower than those observed during room temperature rubs, but the lower forces did not always result in proportionately reduced blade wear.

- Substrate temperatures measured during rubs could be misleading when making sample-to-sample comparisons because of differences in rub path lengths and depths caused by variances in scabbing and blade wear.

- The Phase I materials can be grouped into three basic categories based on rub behavior: a) Al and Zn which produced smooth rub paths and no blade wear; b) Cu-base alloys (except for Cu-9Al hot rub) which produced rough, scabbed rub surfaces and blade wear; and c) Fe and Ni-base alloys which produced blade wear but only light scabbing.

4.2.1.3 Coating Appearance and Microstructure

Al and Zn Coatings

1) The coatings were densified in areas beneath and adjacent to the rub path.

2) Heavy plastic deformation was obvious in both coatings. Subsurface flow lines were visible even without etching.

3) No blade metal was transferred to the coating surface.

Cu-base Coatings

1) The coatings were densified in areas beneath the rub path.

2) Significant amounts of blade metal transferred to the coating surface (scabbing).

3) Although the rub surfaces were oxidized, oxidation of the coating beneath the rub paths was minimal.

4) Cracking (probably thermal) was evident in the scabbed areas (Figure 5).

5) The blade tips were heavily burred on the edges indicating plastic deformation of the blades (Figure 6).

6) Reactions between the transferred blade metal and the coating were evident in the variety of phases present in the microstructure of the scabbed areas (Figure 7). The reaction zones of Cu-5Al and Cu-9Al coatings were primarily at the edges and corner of the rub paths where scabbing usually initiated. Microprobe analysis normal to the surface and under the rub paths indicated that the phases found ranged in composition from pure coating to pure blade metal. The Cu/Ti ratios in the intermediate regions were similar to that of the Cu-Ti eutectic. Exact phase identification was not attempted since the coating-blade metal mixtures were quaternary alloys with unknown phase diagrams.

7) The as-sprayed and annealed coatings had lamellar structures typical of thermally sprayed materials. After rubbing, the Cu-5Al coating showed evidence of recrystallization and twinning, but the lamellar structure was still present (Figure 8). The lamellar structure was absent in the Cu-9Al coating after rubbing (Figure 9). The grain size of the coating was smaller and more uniform than the Cu-5Al coating indicating that extensive cold working and recrystallization had occurred during the rub.

Fe and Ni-base Coatings

1) The coatings were densified beneath the rub paths.

2) Only light scabbing was evident.

3) Cracking (probably thermal) of the coatings occurred perpendicular to the rub direction (Figure 10).

4) The blade tips were burred indicating plastic deformation during the rub (Figure 11).

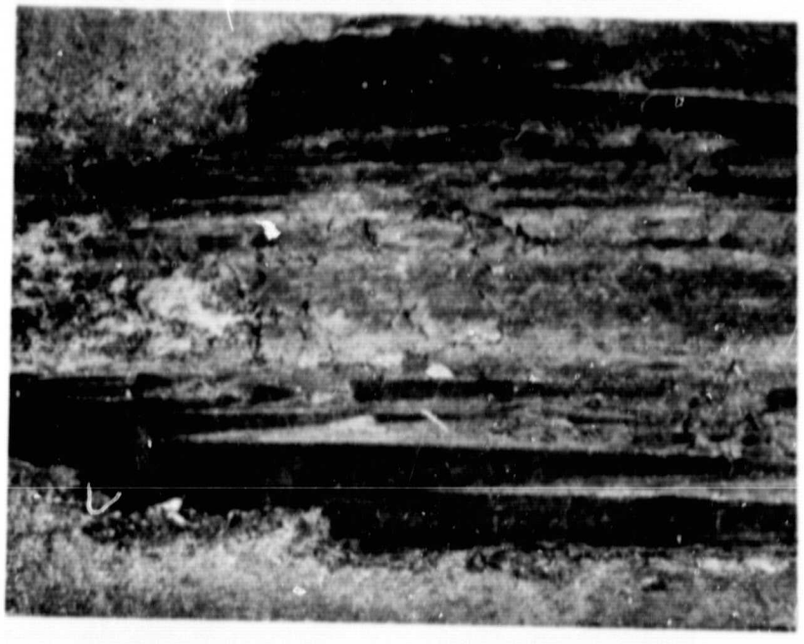

10X

Figure 5. Thermal cracking in scabbed area of Cu coating - Cold rub

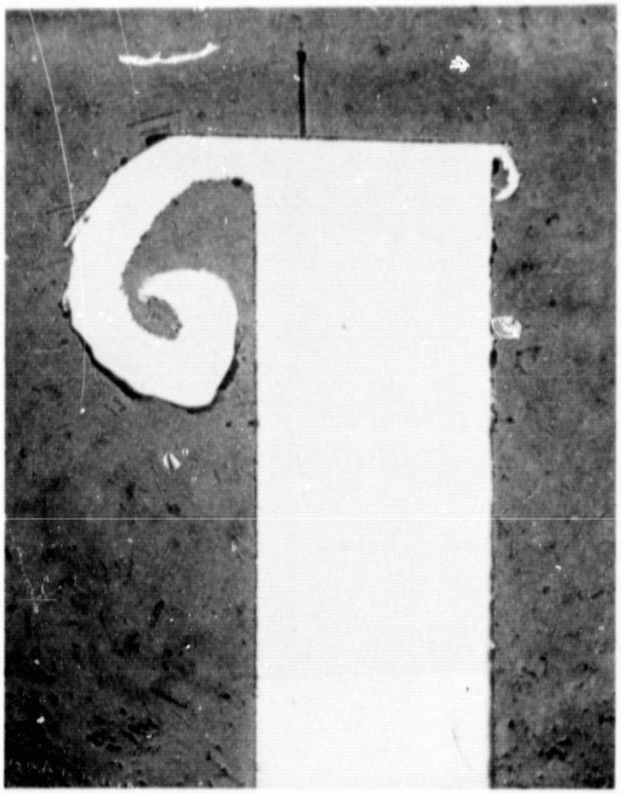

50X

Figure 6. Burring of Ti-6-4 blade used for cold rub of Cu

Figure 7. Microstructure of Cu coating (hot rub) in a scabbed area showing the variety of phases present

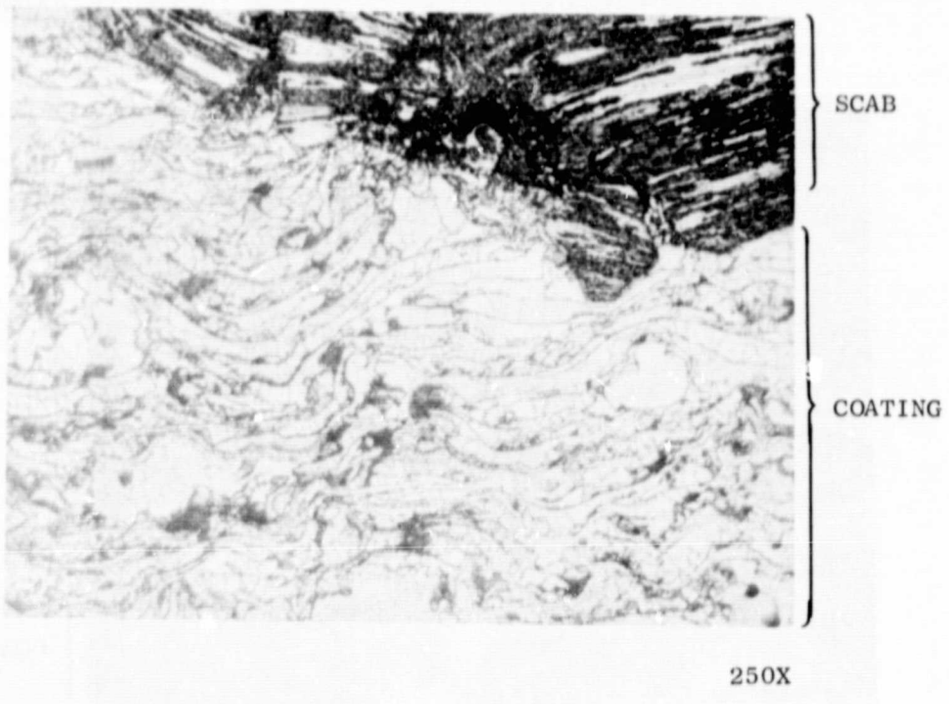

Figure 8. Microstructure of Cu-5Al coating (hot rub) in scabbed area showing the lamellar nature of the coating and the scab (upper right)

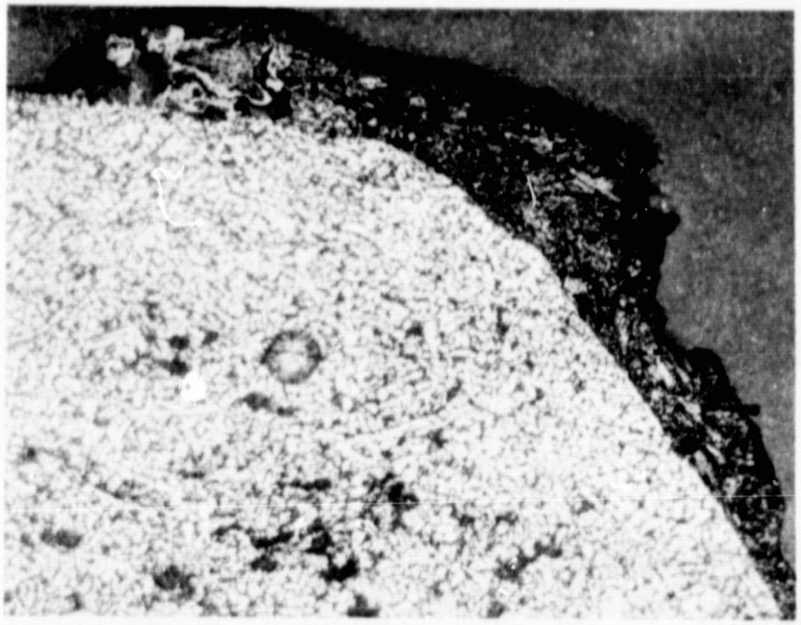

250X

Figure 9. Microstructure of Cu-9Al (hot rub) near edge of rub path showing a light scab and the non-lamellar nature of the coating

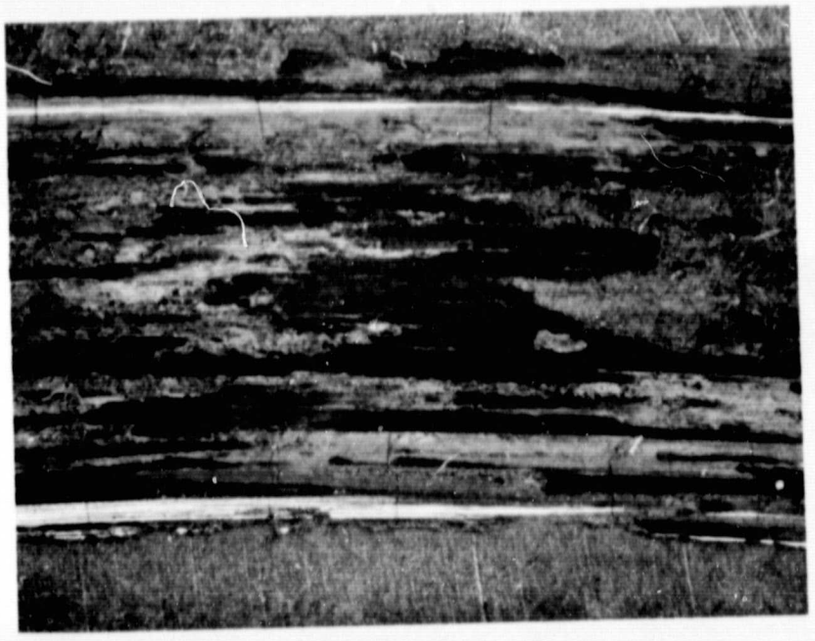

(a) Fe-13Cr

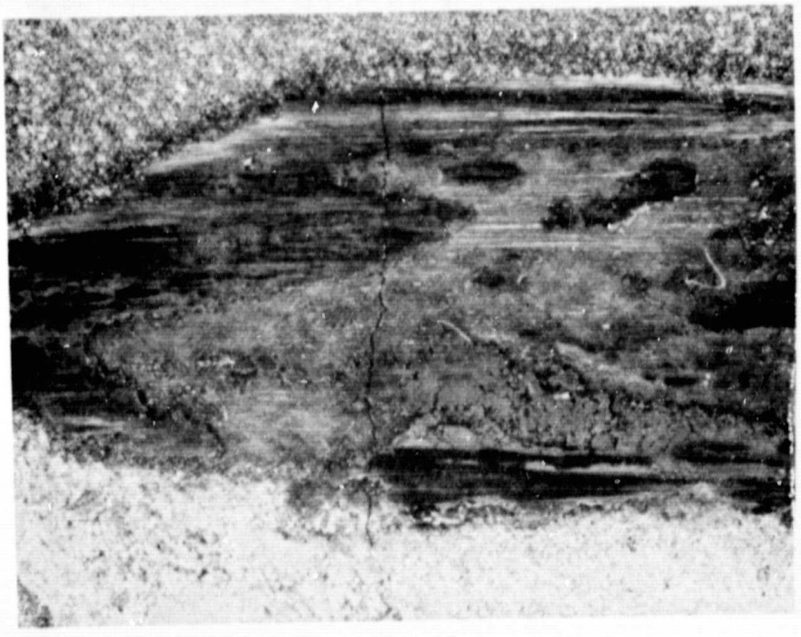

(b) Ni-13Cr

Figure 10. Thermal cracking of Fe-13Cr and Ni-13Cr cold rubs. Cracks are perpendicular to rub direction.

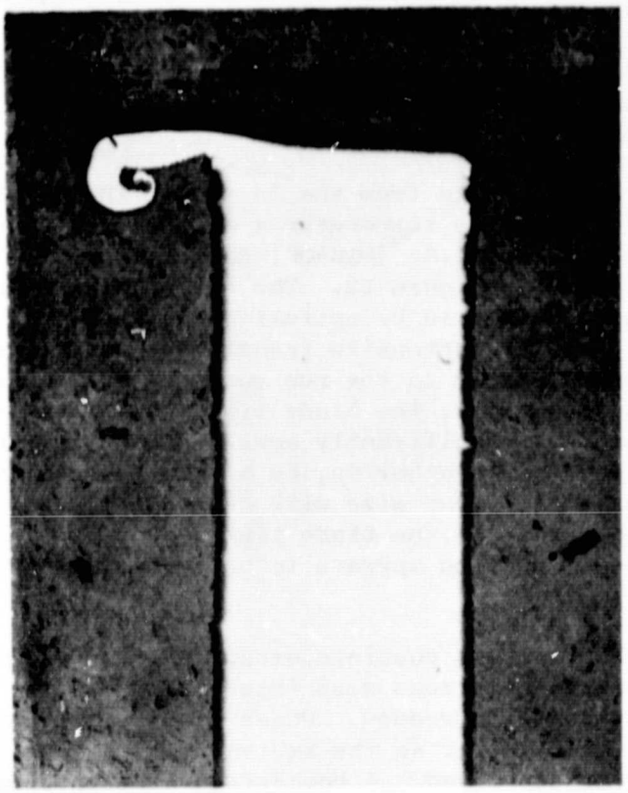

10X

Figure 11. Burring in a Ti-6-4 blade used in Fe-cold rub which was typical of Fe and Ni base coatings

5) Reaction zones were evident in the coatings similar to, but less extensive than, those of the Cu-base coatings. As with the Cu-base alloy, microprobe examination revealed that the Fe/Ti ratios in the intermediate regions were close to that of the Fe-Ti eutectic.

4.2.1.4 Blade Microstructures

EDAX (Energy Dispersive X-ray) analysis in the Scanning Electron Microscope of blade tips from the Cu, Cu-10Zn, Cu-9Al and Fe rubs indicated that for the Cu-9Al and Fe rubs, significant coating material was transferred to the blade tip while the blades rubbed against Cu and Cu-10Zn were clean.

All blade tips except those from the Zn and Al (hot) rubs contain martensite, indicating that the temperatures of the tips exceeded the β-transus temperature of Ti-6Al-4V (≈1840F) during the rubs. A typical etched blade tip is shown in Figure 12. The extent of the martensite zones could be readily determined by optical microscopy, and measurements of the linear depth of martensite transformation in the blade tips (in the direction perpendicular to the rub surface) are compiled in Table 4. As shown in the table, the blade tips from Cu-9Al rubs exhibit martensite zones which are significantly smaller than the zones associated with rubs of any of the other Cu, Fe or Ni-base coatings. Assuming that the martensite zone size will be proportional to the highest temperature attained at the blade tip/rub surface interface during a rub, the Cu-9Al coating appears to be producing lower rub temperatures.

Table 4 shows that for all coatings except Al and Cu-5Al there is a clear increase in martensite zone size (blade tip temperature) as the ambient test temperature is increased. Phase I rub test data (Table 3) showed that for a given material as the ambient test temperature was increased, the rub energy decreased. A comparison of data from Tables 3 & 4 leads to the conclusion that in most cases the reduction in rub energy with increased temperature (ambient test or blade tip) may merely be a reflection of the general inverse flow stress/temperature relationship of most materials. In the case of the weaker coatings (Al and Zn), the flow stress of the coatings would be expected to drop more rapidly with temperature than the flow stress of the Ti 6-4 blades. In the case of the stronger coatings (Cu, Fe and Ni-base) the extreme temperature sensitivity of the flow stress of Ti 6-4 at temperatures above 1000F may be the dominant factor. This general type of behavior would explain why low energy rubs cannot always be expected to produce low blade wear. Unfortunately, improved rub coatings cannot be identified on the basis of elevated temperature mechanical properties alone since it has become evident that in many cases metallurgical reactions can occur during rubs.

4.2.1.5 Property Considerations

Property differences between Cu and Cu-Al alloys have been examined in an effort to identify key features which might account for the

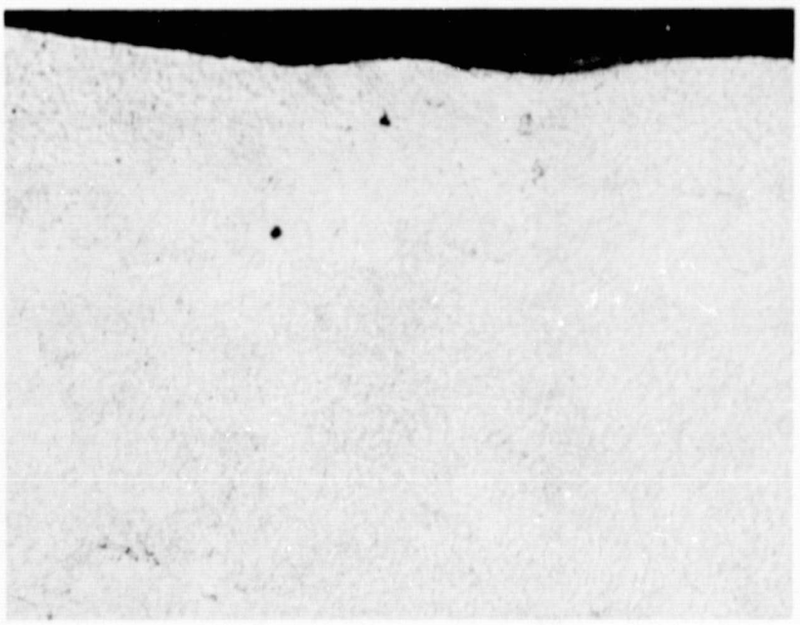

250X

Figure 12. Structure of Ti-6-4 blade tip from room temperature rub of Fe coating showing complete transformation to martensite

TABLE 4

MARTENSITE TRANSFORMATION DEPTHS

Rub Coating	Ambient Test Temp. (Room Temp. or Hot)	Depth of Martensitic Zone at Blade Tip (mm)	
		min.	max.
Zn	RT	0	0
Al	RT	0	<0.1
Al	Hot	0	0
Cu	RT	0.5	0.6
Cu	Hot	1.0	1.2
Fe	RT	0.7	0.8
Fe	Hot	1.3	1.4
Cu-5Al	RT	0.6	1.1
Cu-5Al	Hot	0.4	0.9
Cu-9Al	RT	0	0.3
Cu-9Al	Hot	0	0.4
Cu-10Zn	RT	0.3	0.6
Cu-10Zn	Hot	0.5	0.9
Fe-6Al	RT	0.8	0.9
Fe-6Al	Hot	1.1	1.2
Fe-13Cr	RT	0.8	1.1
Fe-13Cr	Hot	1.5	1.7
Ni-13Cr	RT	0.2	0.3
Ni-13Cr	Hot	1.4	1.6

improvement in rub behavior produced by Al additions to Cu. Selected properties of the Phase I materials are compiled in Table 1. As shown in the table, the primary property differences between Cu and Cu-Al alloys occur for melting point, thermal conductivity, tensile and yield strength, hardness, recrystallization temperature, stacking fault energy and impact strength. It should be noted that the bulk material properties will apply to spray coating materials on a microscopic basis, but that on a macroscopic basis, coating properties such as tensile strength, hardness and thermal conductivity will be lower than bulk properties due to the lamellar structure and porosity associated with spray coatings.

Possible effects of the property differences on the rub behavior of coatings are discussed below:

- Thermal conductivity, melting point - The lower thermal conductivities of the Cu-Al alloys as compared to pure copper would be expected to produce hotter rubs due to the decreased ability of the coatings to conduct frictionally generated heat away from the rub paths. The rub and microstructural data showed that temperatures reached by Cu-Al coatings and substrates directly beneath the rub paths were higher than those reached by Cu coatings, but temperatures reached by blade tips during rubs (martensite zone size) indicated that the actual rub surfaces of the coatings may have been hotter than the rub surfaces of the Cu-Al coatings. These data are consistant because the Cu coatings would be able to conduct more heat away from the rub path in lateral directions, resulting in lower temperatures directly beneath the rub path.

  There has been some evidence that high speed sliding contact between two materials may result in the formation of a thin molten layer at the rub interface which can act as a lubricant to reduce the friction coefficient and subsequent wear damage[20]. If this phenomenon had occurred during the rub tests, the temperatures reached by blade tips would have been proportional to the melting points of the coating materials. Blade tip temperatures, as indicated by martensite zone size, reached during rubs of Cu, Cu-5Al, and Cu-9Al coatings were in the same order as the melting points of the coatings(Table 5), and examination of the blade tips and coatings revealed that some melting had taken place (complicated by eutectic reations). However, Cu-10Zn, which has the same melting point as Cu-9Al and a lower thermal conductivity than Cu, did not show any significant improvement over Cu when rubbed, indicating that the improved rub behavior of Cu-Al alloys cannot be attributed solely to melting point and thermal conductivity differences.

- Tensile strength, yield strength, hardness - The higher tensile and yield strengths and hardnesses of the Cu-Al alloys show that these materials are stronger and more difficult to plastically deform than Cu. Because of their higher strengths, Cu-Al alloys would be expected to require more force (energy) for deformation, and rub force (shear) data from Phase I tests show that higher forces were generated during rubs of Cu-Al alloys. However, Cu

TABLE 5

MELTING POINT/MARTENSITIC DEPTH RELATIONSHIPS

Coating	Coating Melting Point (°F)	Martensite Depth In Blade Tips in mm
Cu	1983	1.0-1.2
Cu-5Al	1940	0.4-0.9
Cu-9Al	1908	0.0-0.4

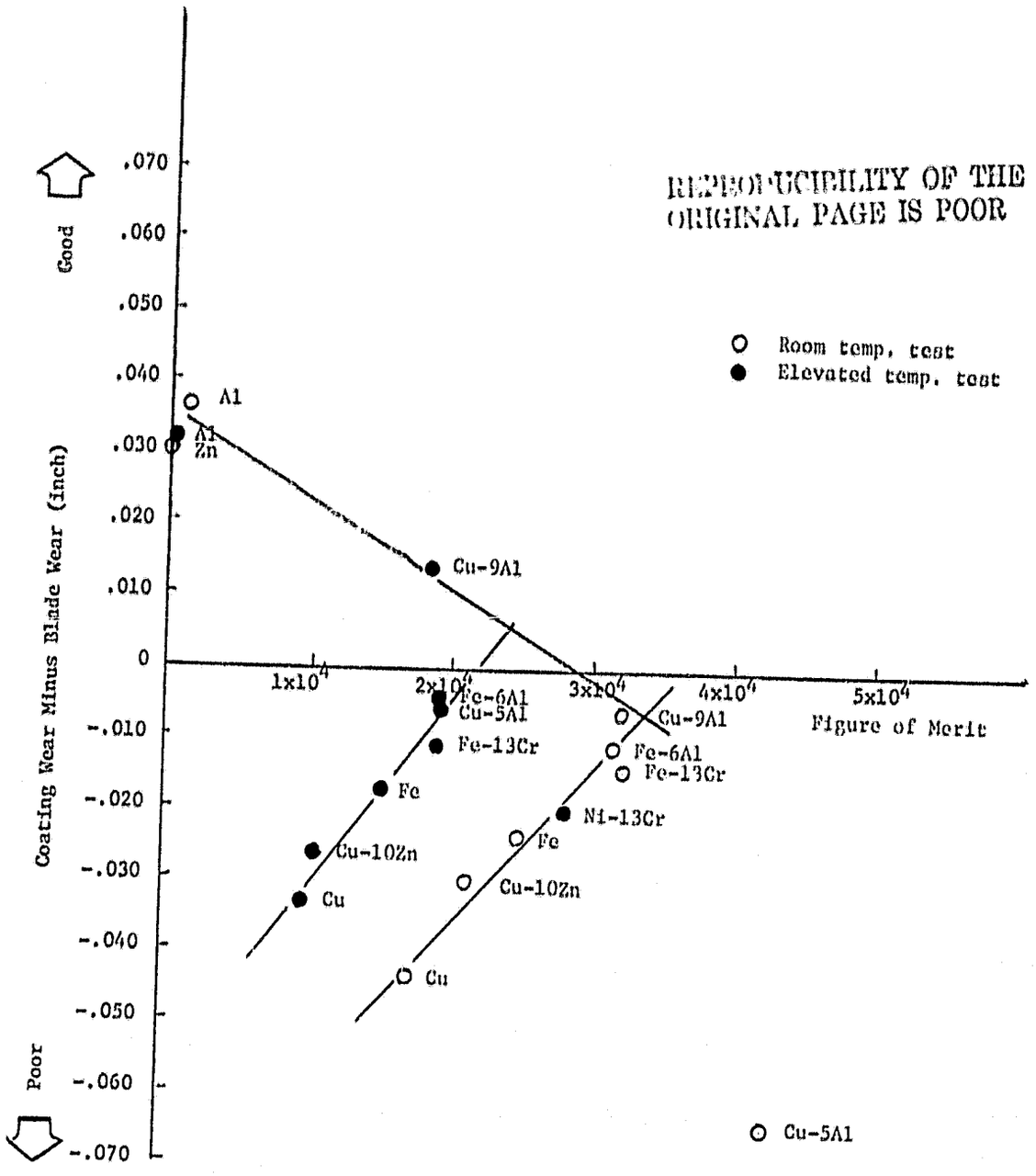

Figure 13. Rub Performance Versus "Figure of Merit"

rubs caused more blade wear than Cu-9Al rubs, indicating that mechanical strength differences cannot account for the improved rub behavior of Cu-Al alloys.

- Recrystallization temperature, stacking fault energy - The recrystallization temperatures and stacking fault energies of Cu and Cu-Al alloys are significantly different. However, the combined effects of these properties (along with recrystallization, work hardening and recovery rates) result in good hot working characteristics and hot working temperature ranges (1400-1700) which are similar for both Cu and Cu-Al alloys, indicating that general hot working characteristics are not obvious causes of the observed differences in rub behavior.
- Impact strength - Impact strength is the only mechanical property examined that indicates Cu-Al coatings should behave differently than both Cu or Cu-12Zn coatings. As shown in Table 1, the impact strengths of Cu and Cu-10Zn are approximately 2 to 3 times as large as the impact strength of Cu-9Al (at room temperature). Since impact testing imposes high strain rates (10^3/sec) on materials and rub test blades "impact" a coating at high speeds, it is possible that a dense coatings response to shock loading may be an important factor in rub behavior.

In summary, examination of the rub test, metallographic and physical property data from Phase I materials revealed no obvious key features for abradable, high melting point materials, although Al additions to Cu improved the rub behavior of dense spray coatings.

R. C. Bill has proposed a "Figure of Merit" to rank rub performance of materials based on the adiabatic heating of seal materials by rub induced deformation until hot working temperature range is reached.

$$\text{Figure of Merit} = (\text{Tensile Strength}) \times (\text{Elongation}) \times \rho Cp \times (T_{hw} - T_{amb})$$

where:
- ρ = density
- Cp = specific heat
- T_{hw} = hot working temperature
- T_{amb} = ambient temperature

The "Figure of Merit" was calculated for each of the coatings using the properties listed in Table 1 and plotted against a rub performance factor (coating wear minus blade wear) for each test in Figure 13. It appears that the rub performance of the materials do show some correlation with the "Figure of Merit" but that different wear mechanisms are indicated dependings on the degree of abradability/abrasivness of the coating.

Several areas which warrant further attention have been identified:

1) The apparent ability of Al additions to Cu to reduce Cu-Ti eutectic reactions during rubs.
2) The potential for easy plastic deformation of near-eutectoid Cu-Al alloys.
3) The potential for surface melting/lubrication during rubs.
4) The role of impact behavior on a material's response to high velocity rubs.
5) "Figure of Merit"/rub performance correlations which include the blade material properties and heat partitioning between coating and blade.

TABLE 6

PHASE II RUB TEST COATINGS

Plastically deformable coatings

Al (dense plasma sprayed)

Low cohesive strength abradable coatings

Metco 601 Aluminum Bronze/Nickel Grahpite (AlBr/NiCg) 80/20 Nickel Graphite (NiCg)	(Porous thermal sprayed)
AB-1 Feltmetal 515B	(Porous sintered)

Modified Phase I coatings

Plasma sprayed Al over Feltmetal
Plasma sprayed Al Bronze over Feltmetal

4.2.2 Phase II - Current Compressor Clearance Coatings

4.2.2.1 Material Selection and Preparation

There are two major types of compressor clearance coatings currently in use. They are: a) the easily plastically deformed coatings; and b) the low cohesive strength coatings. Table 6 lists the coatings used for Phase II rub testing.

Plasma sprayed Al was chosen as an example of a plastically deformable coating currently in use. The low cohesive strength coatings were chosen to cover a wide range of abradability among the current compressor coatings.

The Feltmetal underlayer was added to some of the Phase I coatings to study the effect of a compliant layer underneath the rub coatings. The Feltmetal pad has a low thermal conductivity due to its high porosity, and this effect on the rub of the coatings was also to be assessed.

4.2.2.2 Rub Test Results

The results of the rub tests of Phase II coatings are in Table 7.

Only two materials, AlBr/NiCg and 80/20 NiCg, caused blade wear. Microstructural examination of these coatings revealed that the rub surfaces of the samples which caused blade wear were compacted to various degrees during the rubs (Figure 14 and 15). The 80/20 NiCg cold rub specimen which did not wear blades did not have a compacted surface. Some surface compaction also occurred in Feltmetal 515B specimens (Figure 16); however, the compaction was less than that observed for AlBr/NiCg and 80/20 NiCg specimens, and the FM 515B specimens did not wear blades.

The lowest rub forces were observed for the Metco 601, AB-1 and Al/Feltmetal rubs. The highest rub forces were produced during AlBr/NiCg and 80/20 NiCg rubs where blade wear occurred, but the force associated with the cold Al rub, which did not wear blades, was also high. The rub energies calculated from the rub force-time curves appear to support the Phase I observation that rub force/energy and blade wear do not correlate with respect to different materials. Even when rub energy has been adjusted on a unit volume basis (last column of Table 7) there are no obvious trends to the blade wear and rub energy data except that the denser Phase II materials (Al, AlBr/NiCg and 80/20 NiCg) cause higher rub force and energy generation in most cases.

The AlBr/NiCg and 80/20 NiCg specimens were the only materials which produced significant substrate temperature rises during both hot and cold rubs. Heat discoloration on the surfaces of these samples was quite obvious. Discoloration also indicated that the rub surfaces of the FM 515B and AlBr/Feltmetal specimens were hotter than the 900F ambient test temperature, but the low thermal conductivity of the Feltmetal caused the substrate temperatures to remain virtually unchanged.

Micro-examination of blade tips revealed only one unexpected feature, approximately one mil of pick-up on blades from the AlBr/Feltmetal rub (Figure 17). The material on the tip is dense and uniform indicating severe deformation or possibly melting took place during the rub. Since Cu-9Al wore blades (Phase I testing) and the AlBr (Cu-9Al-1Fe)/Feltmetal did not, it is apparent that the addition of the Feltmetal layer between the spray coating and the substrate is reducing the severity of rubs.

TABLE 7

PHASE II RUB TEST DATA

Coating	$T_{Ambient}$ (°F)	T_{Max} (°F)	$\Delta T(=T_{Max} - T_{Ambient})$	Max Temp Rise Rate (°F/sec)	Max Shear Force(lbs)	Max Force Rise Rate (lb/sec)	Avg Depth of Rub (inch)	Avg Blade Wear (inch)
Al	115	550	435	198	3.3	3.13	0.027	< 0.001
Al	850	950	100	44.4	1.0	0.226	0.028	< 0.001
Metco 601	100	225	125	43.9	0.41	0.340	0.037	< 0.001
Metco 601	900	900	0	-	< 0.25	-	0.036	< 0.001
AlBr/NiCg	100	875	775	300	4.0	5.7	0.029	0.004
AlBr/NiCg	900	1275	375	175	1.8	2.33	0.023	0.006
80/20 NiCg	120	650	530	215	2.7	1.76	0.026	< 0.001
80/20 NiCg	925	1300	375	290	4.2	4.3	0.017	0.004
AB-1	120	120	0	-	< 0.25	-	0.035	< 0.001
AB-1	900	900	0	-	< 0.25	-	0.029	< 0.001
Feltmetal 515B	100	150	50	19.2	1.5	1.70	0.028	< 0.001
Feltmetal 515B	950	950	0	-	0.9	1.02	0.020	< 0.001
Al/Feltmetal*	100	150	50	15	0.41	0.68	0.031	< 0.001
Al/Feltmetal*	875	875	0	-	< 0.25	-	0.026	< 0.001
AlBr/Feltmetal*	900	900	0	-	0.9	1.65	0.026	0 (1 mil pick-up)

Coating Hardness R_{15Y}	Rub Surface Roughness RMS (micro-inch)	Rub Surface Appearance	Rub Energy (Ft-lbs)	Rub Energy/Unit Volume of Coating Removed (Ft-lbs/in^3)
73	50-60	Smooth, dense	3045	2.26×10^5
73	60	Smooth, dense	692	4.94×10^4
56	>300	Deeply grooved	611	3.30×10^4
55	50-60	Lightly grooved	-	-
74	120-200	Lightly scabbed	5509	3.80×10^5
72	>300	Lightly scabbed	2078	1.81×10^5
57	110-300	Smooth, porous	3112	2.39×10^5
50	300	Lightly scabbed	2613	3.07×10^5
<0	300	Smooth, porous	-	-
<0	180	Smooth, porous	-	-
<0**	70-80	Smooth, porous	1171	8.36×10^4
<0**	100-150	Lightly grooved	693	6.93×10^4
-	-	Lightly grooved	530	3.42×10^4
<0**	50-55	Lightly grooved	-	-
-	-	Smooth, spalled in some areas	607	4.67×10^4

*Specimens prepared by NASA

**Feltmetal too soft for hardness reading

Blade material:	Ti-6Al-4V
Number of blades:	48
Blade thickness:	0.025 inch
Incursion rate:	0.010 inch/sec
Incursion depth:	0.020-0.030
Blade tip speed:	500 FPS

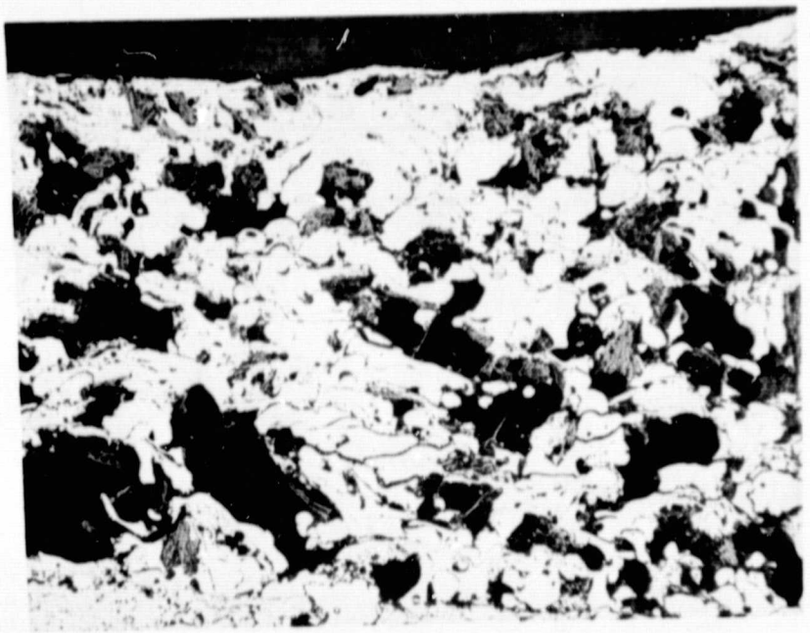

a) Cold Rub 100°F

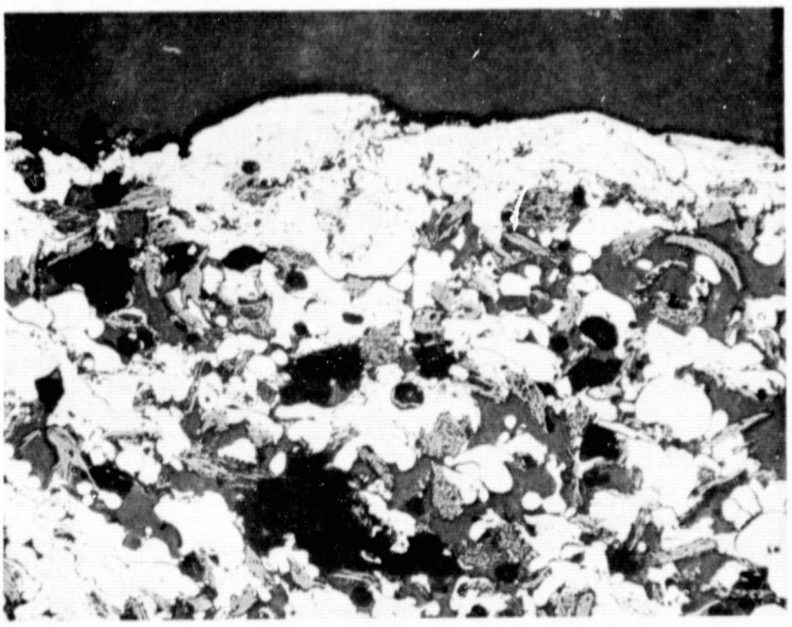

b) Hot Rub, 900°F (100X)

Figure 14. Cross-section of rub paths showing compaction of AlBr/NiCg.

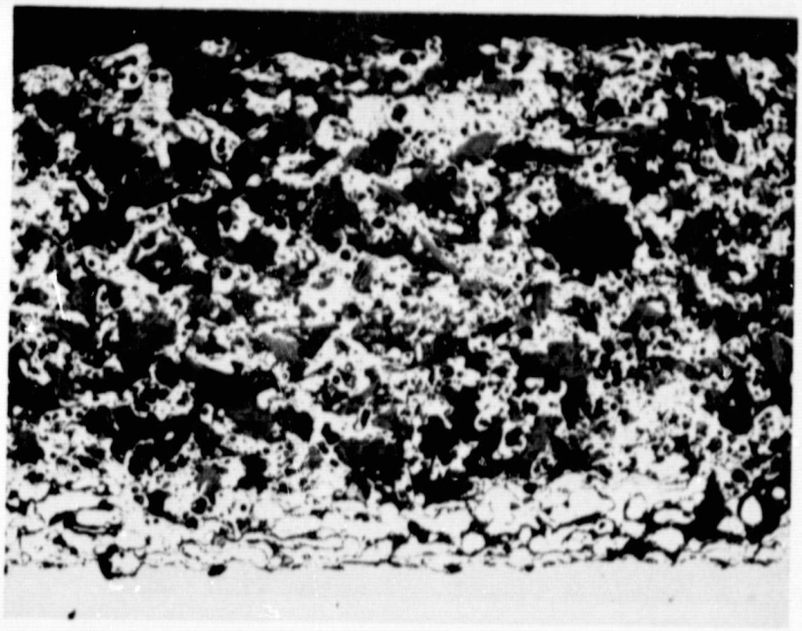

a) Cold Rub, 120°F

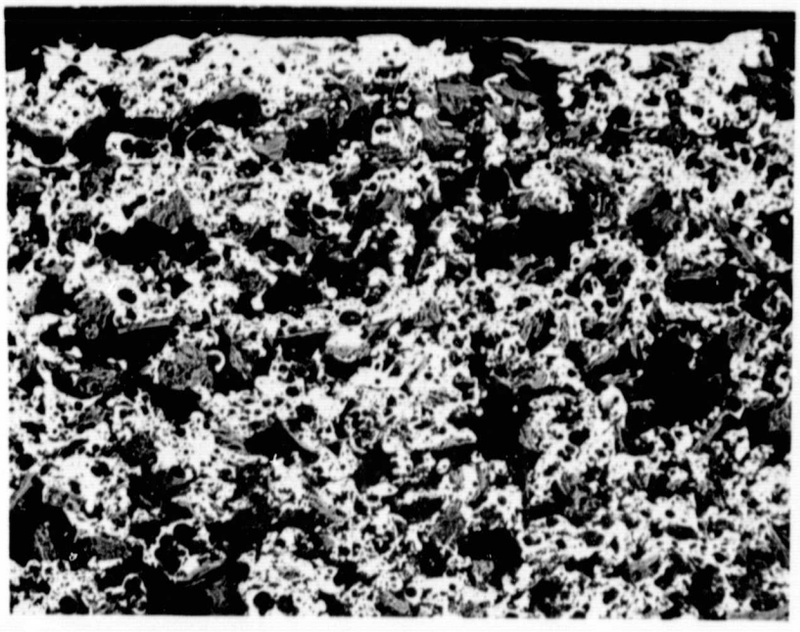

b) Hot Rub, 925°F

(100X)

Figure 15. Cross-section of rub paths of 80/20 NiCg showing compacted and non-compatected surfaces

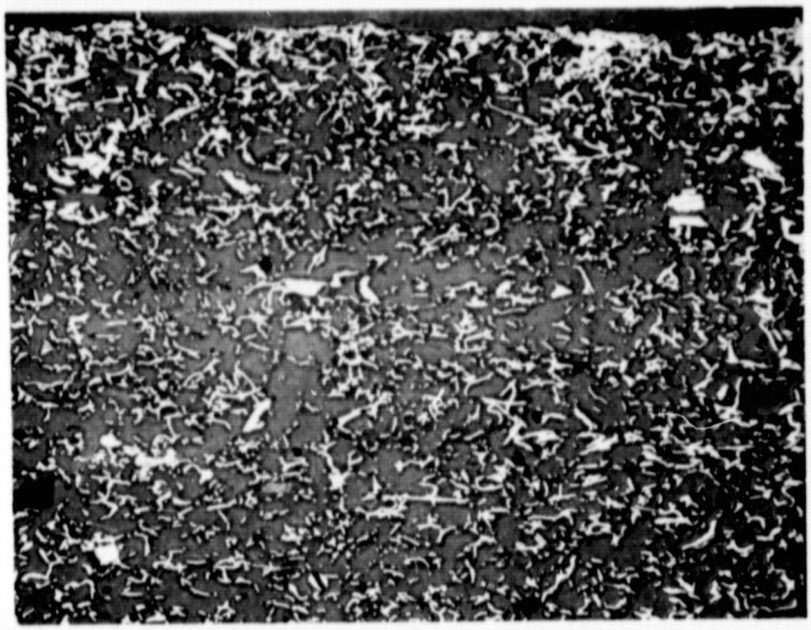

a) Cold Rub, 100°F

b) Hot Rub, 950°F

50X

Figure 16. Cross-sections of rub paths showing minor compaction of Feltmetal 515B

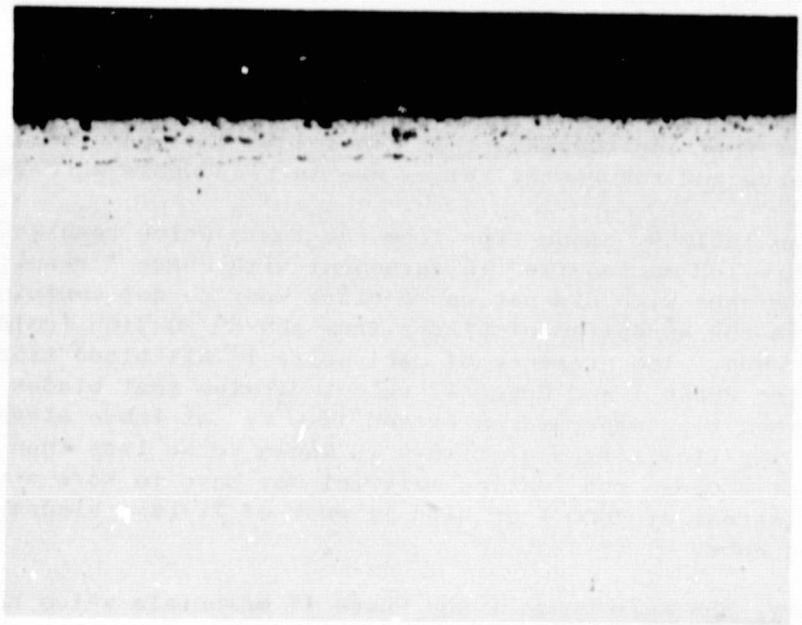

250X

Figure 17. Blade tip from AlBr/Feltmetal hot rub showing uniform pick-up layer of Al/Br

The most unique coating microstructure was that of the Al/Feltmetal and AlBr/Feltmetal materials supplied by NASA. The spray materials on the Feltmetals remained essentially intact during rubs, resulting in smooth, dense rub surfaces with only minor compaction of the supporting Feltmetal (Figure 18.). Approximately one-half of the AlBr spalled from the Feltmetal during the rub, but the remaining material had a smooth finish. The reason for the AlBr spallation has not been established.

A comparison of data from Phase I and Phase II tests on Aluminum (Table 8) shows that for the same test conditions the measured temperature, shear force and rub energy values are in reasonable agreement.

As shown in Table 9, blade tips from rub tests which resulted in blade wear exhibited martensite (in agreement with Phase I results); blade tips from rubs wich did not cause blade wear do not contain martensite with the exception of blades from the 80/20 NiCg (cold) and AlBr/FM (hot) rubs. The presence of martensite in all blade tips which were worn during Phase I and Phase II rubs indicates that blades are wearing only when tip temperatures exceed 1840°F. At these elevated temperatures, the flow stress of Ti-6-4 is known to be less than 5 ksi, indicating that a dense rub coating material may have to have a very low bulk flow stress at 1800°F or high if wear of Ti-base blades is to be avoided during rubs.

In summary, the only Phase I and Phase II materials which have produced the target goals, no blade wear and smooth, dense rub surfaces, are Al and Al/Feltmetal. Cu-9Al, which produced a smooth rub surface during hot rubbing, wore blades, but AlBr(Cu9-Al-1Fe)/Feltmetal produced a rub which did not wear blades. AlBr spalled during the rub, however, indicating that some modification of the AlBr/Feltmetal system might also produce a material capable of providing smooth, dense rub surfaces.

4.2.3 Phase III - Porosity Effects

4.2.3.1 Material Selection and Preparation

Coating wear (depth of rub) minus blade wear was used to rank the rub performance of the Phase I coatings (Table 10) and to select a coating for study of porosity on tub behavior. Cu-9Al ranked the highest of the Cu, Fe, and Ni based coatings. In the case of the Cu-9Al hot rub, a depth of rub and a rub surface similar to pure Al (figure 19) were exhibited.

a) Al/Feltmetal - Cold Rub, 100°F

b) AlBr/Feltmetal - Hot Rub, 900°F 100X

Figure 18. Cross-section of rub paths from metal spray/Feltmetal materials

TABLE 8

Aluminum Rub Test Data

Coating	$T_{Ambient}$ (°F)	T_{Max} (°F)	ΔT ($T_{Max} - T_{Amb}$) (°F)	Max Shear Force (lbs)	Avg Depth of Rub (inch)	Avg Blade Wear (inch)	Rub Surface Roughness RMS (micro in)	Rub Energy (Ft-lbs)	Rub Energy/Unit Volume of Coating Removed ($Ft\text{-}lbs/in^3$)
Al (Phase I - annealed)	75	640	565	2.3	0.036	<0.001	50-60	2730	1.52×10^5
Al (Phase I - annealed)	855	855	0	1.5	0.032	<0.001	-	714	4.46×10^4
Al (Phase II - as-sprayed)	115	550	435	3.3	0.027	<0.001	50-60	3045	2.26×10^5
Al (Phase II - as-sprayed)	850	950	100	1.0	0.028	<0.001	60	692	4.94×10^4

TABLE 9

MARTENSITE TRANSFORMATION DEPTHS

Rub Test	Blade Wear (Inch)	Depth of Martensite Zone at Blade Tip (mm)	
		Min	Max
Al (cold)	< 0.001	0	0
Al (hot)	< 0.001	0	0
Al/FM (cold)	< 0.001	0	0
Al/FM (hot)	< 0.001	0	0
AlBr/NiCg (cold)	0.004	0.4	0.5
AlBr/NiCg (hot)	0.006	1.0	1.1
AlBr/FM (hot)	1 mil pick-up	0.1	0.5
80/20 NiCg (cold)	< 0.001	0.4	0.5
80/20 NiCg (hot)	0.004	0.9	1.1
FM515 (cold)	< 0.001	0	0
FM515 (hot)	< 0.001	0	0
AB-1 (cold)	< 0.001	0	0
AB-1 (hot)	< 0.001	0	0
Metco 601	< 0.001	0	0
Metco 601	< 0.001	0	0

TABLE 10

RUB PERFORMANCE RANKING - Phase I Coatings

Ranking	Coating	Coating Wear-Blade Wear
1	Al (C)	.036
2	Al (H)	.031
3	Zn (C)	.030
4	Cu-9Al(H)	.014
5	Fe-6Al(H)	-.004
6	Cu-9Al(C)	-.006
6	Cu-5Al(H)	-.006
8	Fe-6Al(C)	-.011
8	Fe-13Cr(H)	-.011
10	Fe-13Cr(C)	-.014
11	Fe (H)	-.017
12	Ni-13Cr(H)	-.020
13	Fe (C)	-.023
14	Cu-10Zn(H)	-.026
15	Cu-10Zn(C)	-.030
16	Cu (H)	-.033
17	Cu (C)	-.044
18	Cu-5Al (C)	-.064

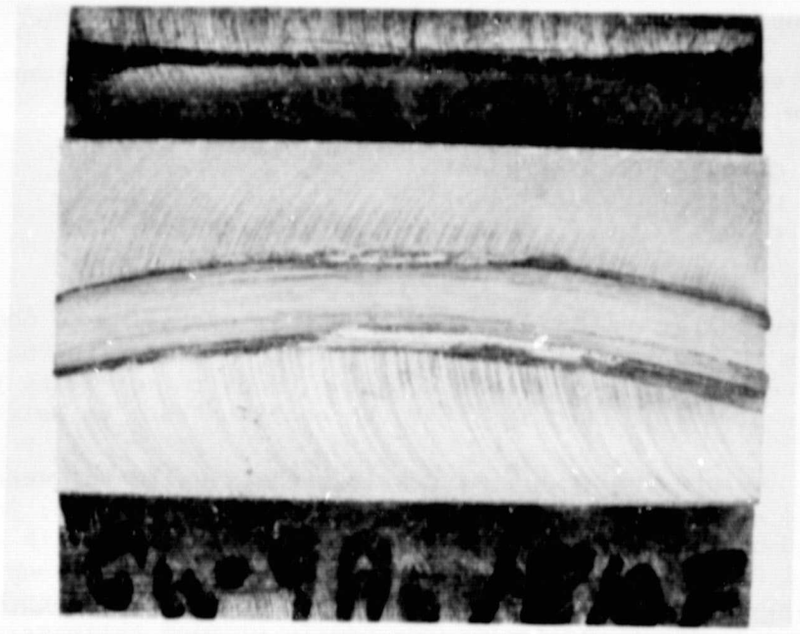

a) Al

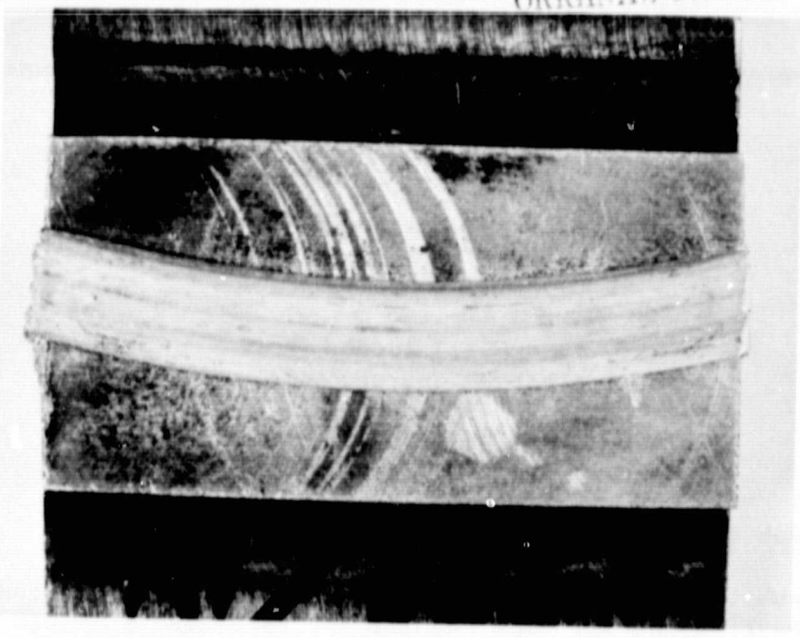

b) Cu-9Al

2X

Figure 19. Comparison of Cu-9Al rub surface and the Al rub surface from hot rubs

Phase II results indicated that a Feltmetal layer under sprayed AlBr coatings tended to reduce blade wear.

Based on the above reults, the following coating systems were selected to study the effect of porosity on rub behavior:

(1a) Cu-9Al + 20 v/o Ekonol
(1b) Cu-9Al + 40 v/o Ekonol
(2a) Cu-9Al + 20 v/o Ekonol/Feltmetal 515B
(2b) Cu-9Al + 40 v/o Ekonol/Feltmetal 515B

Ekonol, a polyester powder marketed by Metco Inc. as Metco 600, was selected as the non-metallic component to be sprayed with the Cu-9Al powder to reduce the density of the spray deposit (introduce porosity) since it is similarly used in other rub coatings such as Metco 601.

Prior to spraying, rub test panels without Feltmetal were grit blasted and sprayed with 0.005 inch of Metco 450 bond coat; panels with brazed-on Feltmetal were very lightly grit blasted with an S.S. White Model D air abrasive (dental type) and cleaned ultrasonically in methyl-ethyl-ketone (MEK) to remove any entrapped grit. Approximately 0.035 inch of coating was applied to panels without Feltmetal. The surfaces of the spray coatings were somewhat uneven due to the traverse fixturing and rates used so the surfaces of all coatings were evened by gentle abrasion with 140 grit SiC paper. Final coating thicknesses were 0.030-0.035 inch for panels without Feltmetal and 0.015-0.020 inch for panels with Feltmetal.

The spray parameters used for both the 20% and 40% Ekonol mixtures were:

Gun - Metco 3MB
Console - Avco
Powder Feeder - Plasmadyne
Nozzle - GH
KW - 21 (550 Amp/38 volts)
Powder Port - #1
Spray Distance - 3 inches
Spray Angle - 90 degrees
Spray Rate - 5.5 lb/hr
Primary Gas - Ar (100 CFH/100 psi)
Secondary Gas - H_2 (5 CFH/80 psi)

4.2.3.2 Rub Test Results

The rub test conditions used for Phase III were identical to those used in Phases I and II. The results are tabulated in Table 11.

The following trends were derived from Phase III rub test results:

i) Significant substrate temperature rises occur only when measurable blade wear or pick-up occurs (this generalization is complicated by the low thermal conductivity of Feltmetal).

TABLE III

PHASE III RUB TEST RESULTS

Coating System	$T_{ambient}$ (°F)	T_{Max} (°F)	$\Delta T(=T_{max}-T_{ambient})$	Max. Temp. Rise Rate (°F/sec)	Max. Shear Force (Lbs)	Max. Force Rise Rate (lb/sec)	Avg. Depth of Rub (inch)	Avg. Blade Wear (inch)	Coating Hardness R_{15Y}	Rub Surface Roughness RMS (Micro-inch)	Rub Surface Appearance
Cu-9Al-20% Ekonol	120	750	630	450	2.8	3.7	0.021	0.004	58	150-170	Lightly grooved, scrubbed
Cu-9Al-20% Ekonol	920	1070	150	140	0.64	0.58	0.015	0.002	43	100-300	Smooth, pullout in some areas
Cu-9Al-40% Ekonol	110	140	30	15	<0.25	-	0.028	<0.001	-	-	Smooth, porous, pullout in some areas
Cu-9Al-40% Ekonol	925	925	0	5	<0.25	-	0.016	<0.001	-	-	Porous, pullout in some areas
Cu-9Al-20% Ekonol-Feltmetal	100	200	100	29	2.6	3.2	0.042	0.004 mil pickup on blade tip)	<0*	100-200	Lightly grooved, scrubbed, pullout in feltmetal in some areas
Cu-9Al-20% Ekonol-Feltmetal	910	930	20	12	1.1	2.2	0.016	0(<0.001 pickup on blade tip)	-	-	Smooth (≈150 RMS)
Cu-9Al-40% Ekonol-Feltmetal	100	100	0	0	<0.25	-	0.040	<0.001	<0*	>300	Rubbed into felt
Cu-9Al-40% Ekonol-Feltmetal	910	930	20	9.1	0.42	4.2	0.025	<0.001	<0*	300	Rubbed into felt

*Feltmetal too soft for hardness reading

Blade material: Ti-6Al-4V
Number of blades: 48
Blade thickness: 0.025 inch
Incursion rate: 0.010 inch/sec
Incursion depth: 0.020-0.030
Blade tip speed: 500 FPS

ii) Significant substrate temperature rise rates occur only for Cu-9Al+20% Ekonol specimens.

iii) The highest rub forces are associated with either blade wear or pick-up.

iv) The presence of a Feltmetal underlayer does not cause a significant reduction in rub forces in relation to the spray coating materials.

v) Cu-9Al+20% Ekonol spray coatings with and without the Feltmetal interlayer yielded partially or completely smooth, smeared rub surfaces (≈150 RMS) after 900F rubs (Figure 20).

Metallographic examination of cross-sections of the rub specimens yielded the following information:

i) Cu-9Al+20% Ekonol and Cu-9Al+40% Ekonol coatings with or without the Feltmetal underlayer have not been compacted under the rub paths (Figure 21).

ii) Coatings with the Feltmetal underlayer were not pushed into the felt during rubs.

iii) In smooth, rubbed areas there is only a thin layer of smeared material. At very high magnification, there appear to be some small Cu-Ti eutectic zones in the smeared areas.

iv) Substantial amounts of Ekonol have been lost from hot rub specimens and from areas adjacent to the rub paths of cold rub specimens with Feltmetal interlayers.

Metallographic examination of etched blade tips revealed thin zones of martensite (<0.001") in blade tips from rubs which caused blade wear or pick-up. These zones are much smaller than those observed in blade tips from rubs of CuAl or AlBr materials (no Ekonol) in Phase I and Phase II tests, indicating that tip temperatures were not greatly in excess of the B-transus temperature for Ti6Al4V(≈1840F). It may be postulated that in rubs where scabs are not formed on rub surfaces, the surface temperature during rubs will be limited by the melting point of the rub coating; in the case where scabs are formed, the temperature at the rub surface would be expected to be somewhere between the melting point of the coating and the melting point of Ti6Al4V(3000F) depending on the extent of scabbing.

The pick-up measured by micrometer on blade tips from Cu-9Al+20% Ekonol/Feltmetal rubs was clearly evident microscopically. In addition, minor pick-up not measurable by micrometer was observed on blade tips from Cu-9Al+20% Ekonol rubs, the coating material picked up on the blade tips appeared to have reacted with the blade tips to form a Cu-Ti eutectic. Examination of the blade tips in the SEM and microprobe reveal the presence of Ti (Figure 22) in the pick-up material. The

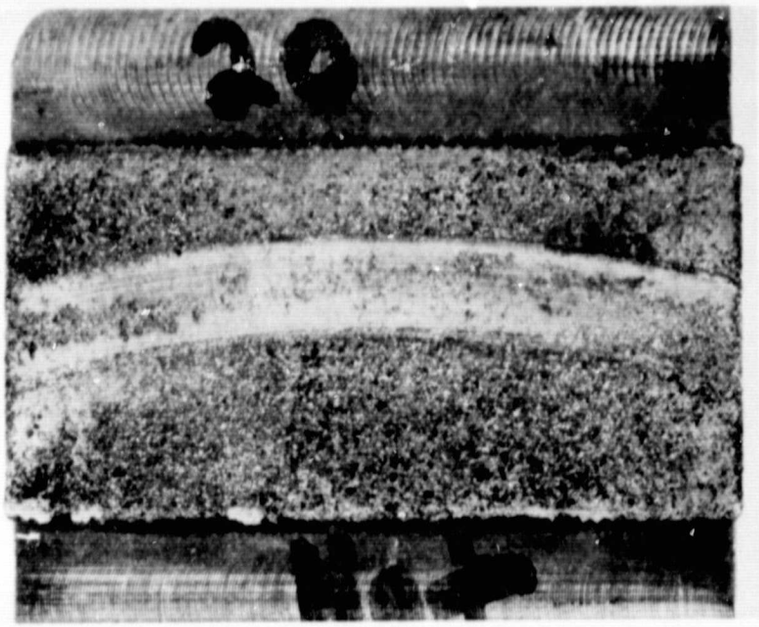

a) Without Feltmetal Underlayer

2X

b) With Feltmetal Underlayer

Figure 20. The hot rub surfaces of the Cu-9Al + 20% Ekonol

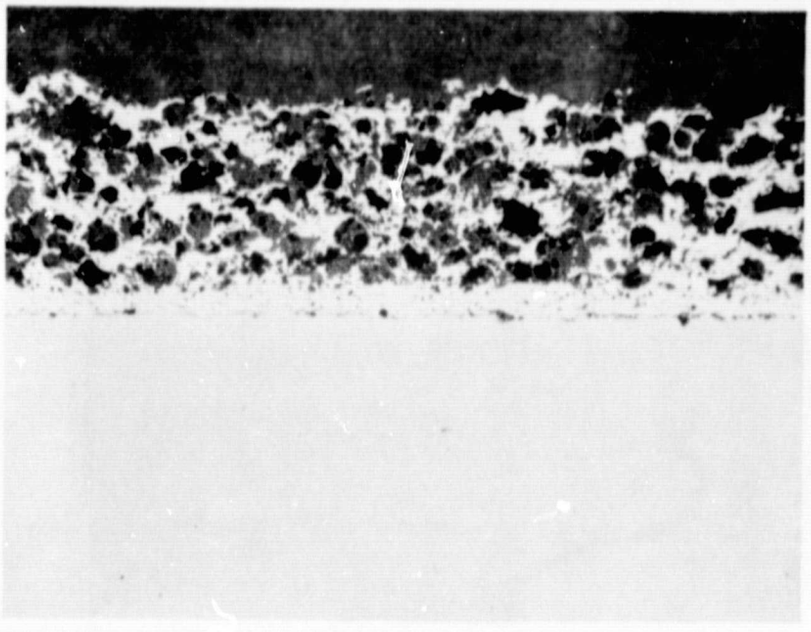

a) Beneath Rub Path

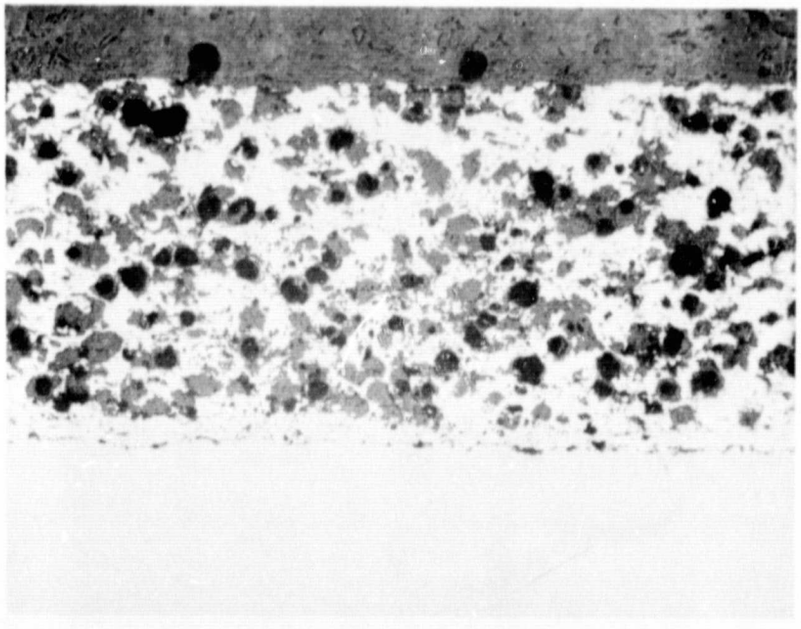

50X

b) Away from Rub Path

Figure 21. Cross-section of Cu-9Al + 20% Ekonol coating

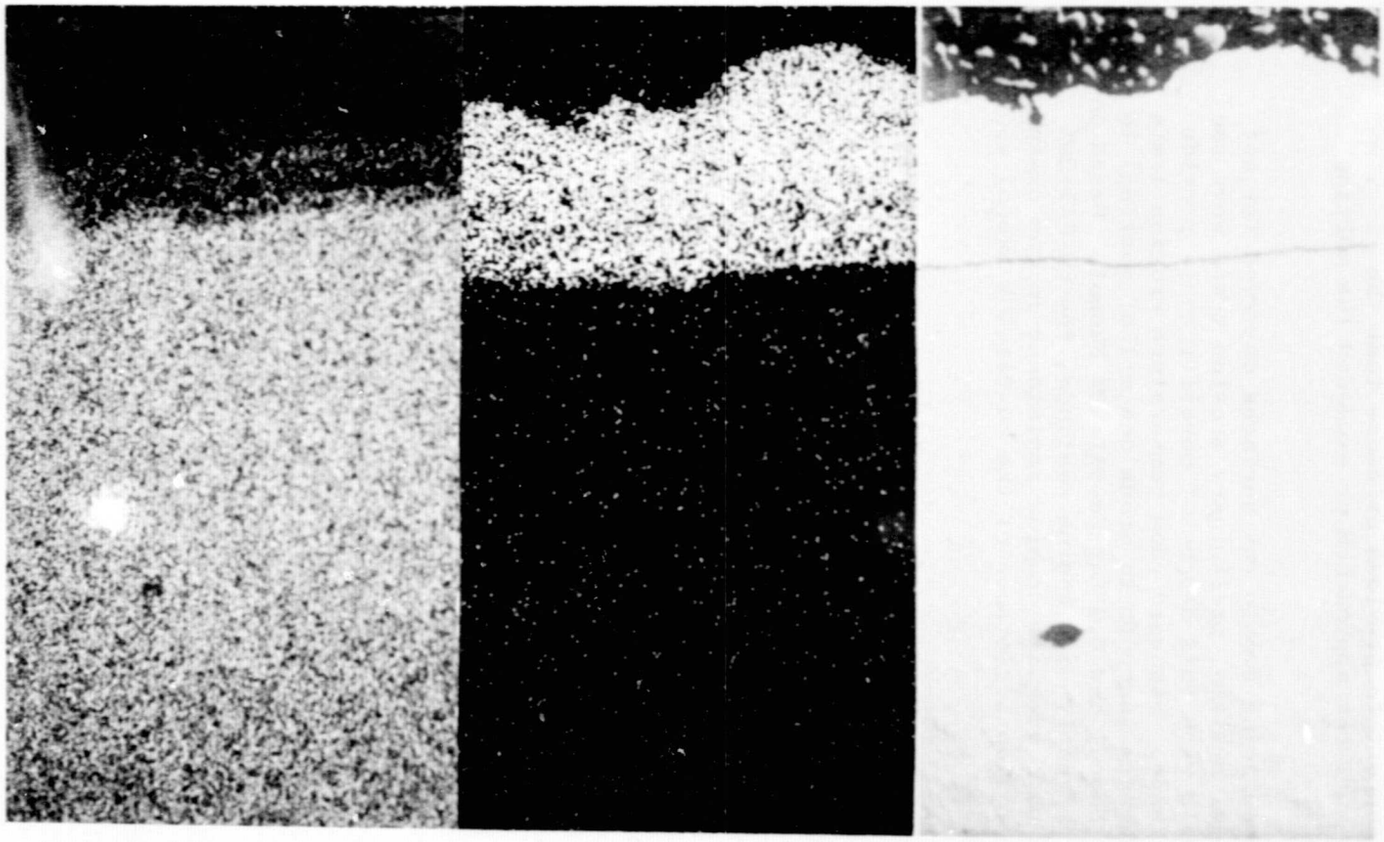

500X

(a)
Backscatter image

(b)
Cu Microporbe scan

(c)
Ti Microprobe trace

Figure 22. Ti6Al4V Blade tip from hot rub with Cu 9Al + 20% Ekonol showing Cu 9Al pickup

presence of detectable amounts of titanium in the coating pick-up would require a significant amount of diffusion to occur during the rub and gives further support to previous evidence that the temperature of the rub surfaces approached or exceeded the melting point of Cu-9Al (≈1910F).

Because of the encouraging smooth rub surfaces observed for hot rubs of Cu-9Al+20% Ekonol systems, preliminary erosion tests were run to determine if materials with this degree of porosity would provide adequate erosion resistance. Standard room temperature erosion tests showed the erosivity numbers (seconds to erode one mil of coating) to be 15.4 for Cu-9Al+20% Ekonol and 6.9 for Cu-9Al+40% Ekonol. Based on erosion resistance of currently used engine coatings, the Cu-9Al+20% Ekonol would appear to have adequate erosion resistance in the as-sprayed condition whereas the erosion resistance of the Cu-9Al+40% Ekonol would be marginal for engines.

The conclusions that can be drawn from evaluation of the Phase III rub data are:

i) The addition of porosity to Cu-9Al coatings significantly reduced blade wear in relation to the wear observed for dense Cu-9Al in Phase I tests.

ii) Cu-9Al+20% Ekonol spray coatings, particularly with a Feltmetal interlayer, have demonstrated the capability for yielding smooth rub surfaces under one set of rub test conditions and have demonstrated erosion resistance which is considered acceptable in relation to spray coatings currently used in engine applications.

iii) Cu-9Al+40% Ekonol coatings are highly abradable. However, they have rougher rub surfaces than Cu-9Al+20% Ekonol coatings, and they have marginal resistance to erosion.

iv) Good rubs of the sprayed Feltmetal specimens cannot be explained by reduced shear forces. The compliance or low thermal conductivity of the Feltmetal may be more important factors than reduced rub forces.

4.3 Task II - Rub Test Parameters

4.3.1 Material Selection and Preparation

Cu-9Al+20% Ekonol with and without the Feltmetal interlayer demonstrated the capability of yielding smooth rub surfaces with a significant reduction in blade wear over the dense coatings coupled with erosion resistance considered acceptable for engine applications. These two coating systems were therefore selected in Task II to determine the effect of rub parameters on their rub behavior.

AlBr (Metco 51F) powder was used in preference to Cu-9Al because of its availability. The nominal composition of Metco 51F is Cu-9.5Al-1Fe. The rub behavior of Metco 51F was expected to be similar to Cu-9Al.

The spray parameters used for the coatings were identical to those previously used in Phase III, Task I.

Prior to spraying, rub test panels without Feltmetal were grit blasted and sprayed with 0.005 inch of Metco 450 bond coat; panels with Feltmetal were very lightly grit blasted with an S.S. White Model D air abrasive (dental type) and cleaned ultrasonically. Approximately 0.030" of the AlBr+20% Ekonol coating was applied to all panels which were sprayed in one operation to insure uniform coating properties.

4.3.2 Test Results

The test parameters selected for study were: a) the incursion rate; and b) the solidity (i.e., number of blades used); and c) the test temperature. Two different incursion rates (0.0001 and 0.001 inch/sec), two solidity variations (48 and 12 blades) and two test temperatures (RT and 900°F) were examined. The remaining test parameters were identical to Task I test parameters.

The test results are listed in Table 12. The following trends were observed from the Task II rub test results:

1) The maximum rub temperatures exceed those observed for 10.0 mil/sec rubs of Cu-9Al+20% Ekonol during Phase III, Task I testing.

2) The maximum shear forces also exceed those observed for 10.0 mil/sec rubs of Cu-9Al+20% Ekonol during Phase III, Task I testing.

3) Some rub force curves show cyclic force vs. time behavior during part or all of the tests.

4) At 0.0001 mil/sec incursion rates, hot rubs are more severe than cold rubs; at 0.001 mil/sec incursion rates, hot rubs are less severe than cold rubs.

5) Twelve (12) blade tests produce more blade wear than 48 blade tests, but maximum temperatures and shear forces are lower for the 12 blade tests.

6) Blade wear for 48 blade tests of AlBr+20% Ekonol is comparable to blade wear observed for Phase III, Task I tests of Cu-9Al+20% Ekonol except for the hot, 0.0001 mil/sec rub, but more scabbing is evident with the AlBr+20% Ekonol.

7) Blade wear is reduced when a Feltmetal underlayer is present.

TABLE 12

TASK II RUB TEST RESULTS

Coating System	Rub Test Parameters* # Of Blades	Incur. Rate ("/Sec)	$T_{ambient}$ (°F)	T_{Max} (°F)	$\Delta T(=T_{Max}-T_{ambient})$	Max. Shear Force (Lbs)	Avg. Depth of Rub (inch)	Avg. Blade Wear (inch)	Coating Hardness R_{15Y}	Rub Surface Roughness RHS (micro-inch)	Rub Surface Appearance
AlBr + 20% Ekonol	48	0.0001	120	850	730	3.4**	0.029	0.033	57	150	Light scabbing
AlBr + 20% Ekonol	48	0.0001	860	1330	470	3.4**	0.011	0.014	48	90-95	Heavy scabbing, light pullout
AlBr + 20% Ekonol	48	0.001	120	800	680	3.0	0.025	0.005	54	150	Light scabbing
AlBr + 20% Ekonol	48	0.001	910	1450	540	2.1	0.013	0.001	70	100-200	Light scabbing
AlBr + 20% Ekonol	48	0.010	880	1280	400	-	0.018	0.006	72	90-100	Smooth, no scabbing
AlBr + 20% Ekonol	12	0.001	110	450	340	2.8**	0.015	0.019	58	100-250	Very light scabbing
AlBr + 20% Ekonol	12	0.001	890	1300	410	1.5**	0.006	0.007	63	80-95	Light scabbing
AlBr + 20% Ekonol + Feltmetal	48	0.0001	110	200	90	2.1**	0.039	0.002	***	>300	Spalled
AlBr + 20% Ekonol + Feltmetal	48	0.0001	880	1090	110	0.4	0.018	0.002	***	35-50	Heavy scabbing with surface cracking
AlBr + 20% Ekonol + Feltmetal	48	0.001	120	220	100	1.7	0.028	0.009	***	150	Moderate scabbing, some pullout
AlBr + 20% Ekonol + Feltmetal	48	0.001	870	950	80	0.8	0.014	<0.001	***	150-160	Light scabbing, moderate pullout

* All other rub test parameters maintained constant for all tests; 0.020" rub depth, 500 SFS tip speed, Ti 6Al-4V blades (0.025" thick).

** Cyclic force vs. time curve.

*** Feltmetal too soft for hardness reading

Blade material: Ti-6Al-4V
Blade thickness: 0.025 inch
Incursion depth: 0.020-0.030
Blade tip speed: 500 FPS

The depth of martensite transformation of the Task II rub blades determined metallographically (Table 13) were larger than those observed in Phase III, Task I, which is in accord with the higher shear forces, amount of blade wear, and maximum rub temperatures observed.

All Task II blades had a uniform pick-up of coating material at the tip (Figure 23) ranging from 0.00005" to 0.0002". Blades with martensite depths of greater than 0.1 mil tended to show heavy burring on the trailing edge but very little coating pick-up on the leading edge. For the blades that had less than 0.1 mil martensite (Figure 24). No burring was observed, and there was coating pick-up on the tip.

The increased temperatures, forces, depth of martensite transformation and scabbing observed for AlBr+20% Ekonol tests with respect to Cu-9Al+20% Ekonol tests could be attributed to the effects of changing incursion rates during tests and/or to a slightly decreased abradability of the AlBr+20% Ekonol. The following evidence points to probable decreased abradability of the AlBr+20% Ekonol as compared to the prior Cu-9Al+20% Ekonol material.

1) The erosivity number (seconds required to erode one mil of coating) of the AlBr+20% Ekonol is ≈20 vs. ≈15 for the Cu9Al+20% Ekonol tested in Phase III, Task I.

2) The microstructure of the AlBr+20% Ekonol. while not grossly different from that of the Cu-9Al+20% Ekonol, shows the AlBr matrix to be slightly denser and more contiguous than the Cu-9Al matrix (Figure 25).

Prior experience with abradable coatings has shown that increased erosion resistance and higher densities will be accompanied by decreased abradability.

The reason for the higher erosion resistance and density of the AlBr+20% Ekonol which was sprayed with the same parameters as the Cu9Al+20% Ekonol is believed to be the finer size distribution of the AlBr (Metco 51F). As shown in Table 14 the size distribution of the AlBr is shifted toward the -325 mesh size range in relation to the Cu9Al size distribution which is centered about the -270 mesh size range. Experience has shown that finer powders can be expected to yield denser coatings if sprayed with similar parameters.

At present, the reasons for the cyclic rub force curves or for the reversal in severity of hot and cold 48 blade rubs when changing from 0.0001 to 0.001"/sec incursion rates are not clear, although the decreased temperatures and rub forces associated with the 12 blade (lower solidity) rubs indicate that a complex relationship between frictional heat generation, thermal conductivity of the coating and possibly windage effects may be a significant factor in observed rub behavior. The effect of incursion rate on amount of blade wear is presented for the 48 blade tests in Figure 26 for both Tasks I and II

TABLE 13

MARTENSITE TRANSFORMATION DEPTHS

TASK II COATINGS

Rub Coating	# of Blades	Incursion Rate (in/sec)	Ambient Test Temp. (Room Temp. or Hot)	Depth of Martensite Zone at Blade Tip (mm)	
				Min.	Max.
AlBr + 20% Ekonol	48	0.0001	RT	0	0
AlBr + 20% Ekonol	48	0.0001	Hot	0	0
AlBr + 20% Ekonol	48	0.001	RT	0	<.1
AlBr + 20% Ekonol	48	0.001	Hot	0	<.1
AlBr + 20% Ekonol	48	0.010	Hot	0	0.1
AlBr + 20% Ekonol	12	0.001	RT	<.1	.1
AlBr + 20% Ekonol	12	0.001	Hot	.1	0.9
AlBr + 20% Ekonol + Feltmetal	48	0.0001	RT	0	<.1
AlBr + 20% Ekonol + Feltmetal	48	0.0001	Hot	<.1	0.2
AlBr + 20% Ekonol + Feltmetal	48	0.001	RT	0	0
AlBr + 20% Ekonol + Feltmetal	48	0.001	Hot	0	0.1

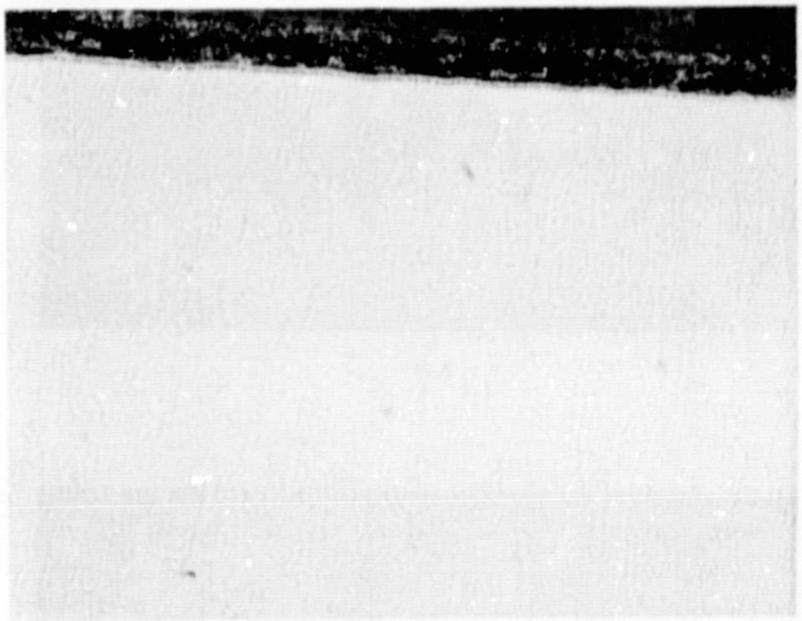

500X

Figure 23. Pick-up coating material on blade tip during cold rub of AlBr + 20% Ekonol with Feltmetal coating, typical of all Task II blades (48 blades, 0.001"/sec incursion rate)

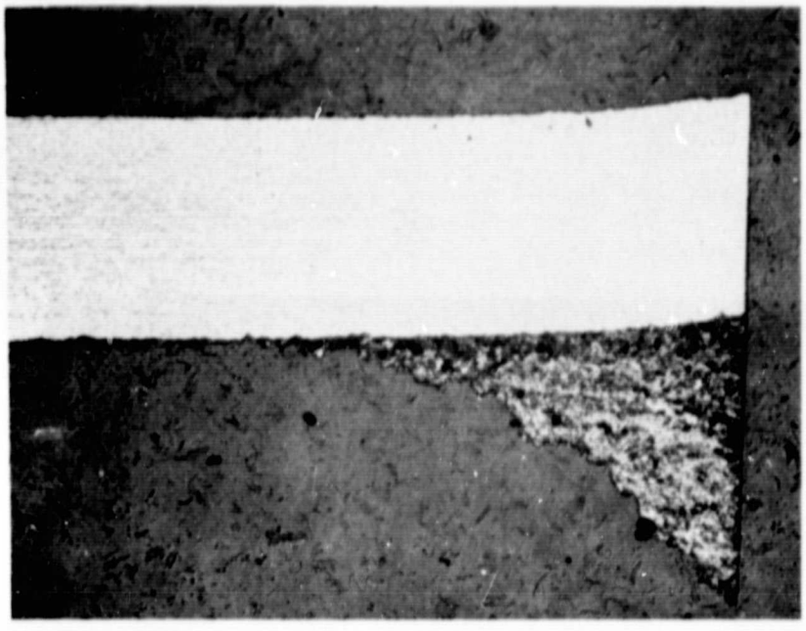

(a)

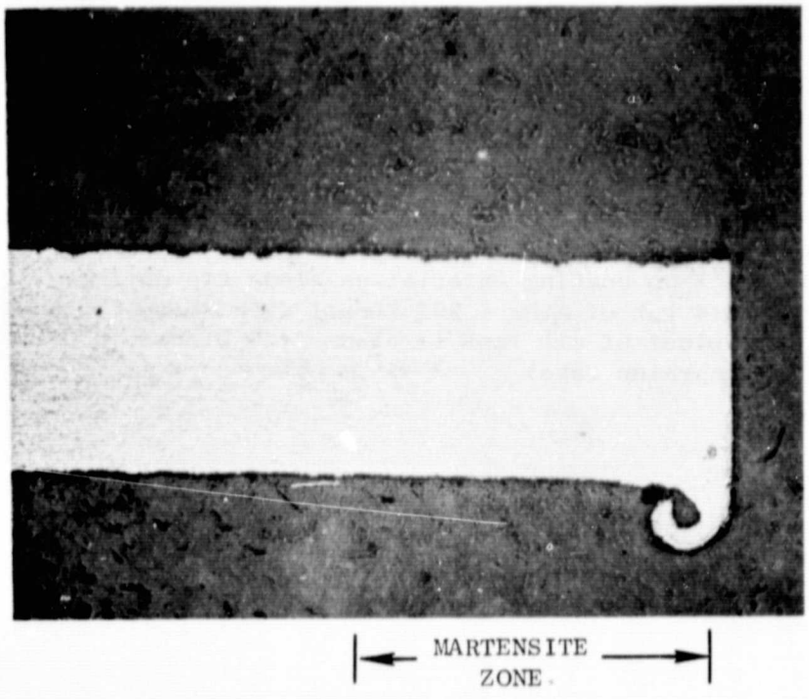

(b)

Figure 24. Ti-6-4 blade appearance for rubs in which a) no Martensite and b) Martensite forms

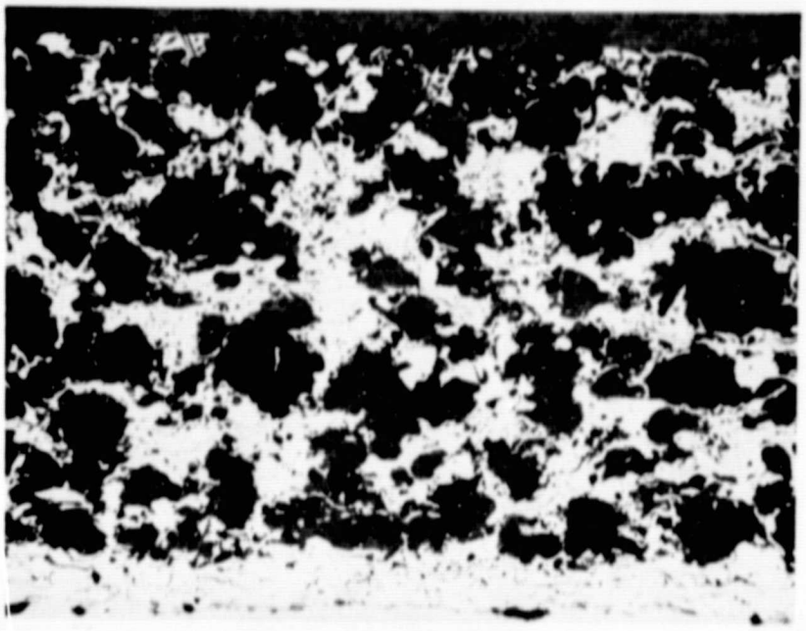

a) Cu 9Al + 20% Ekonol

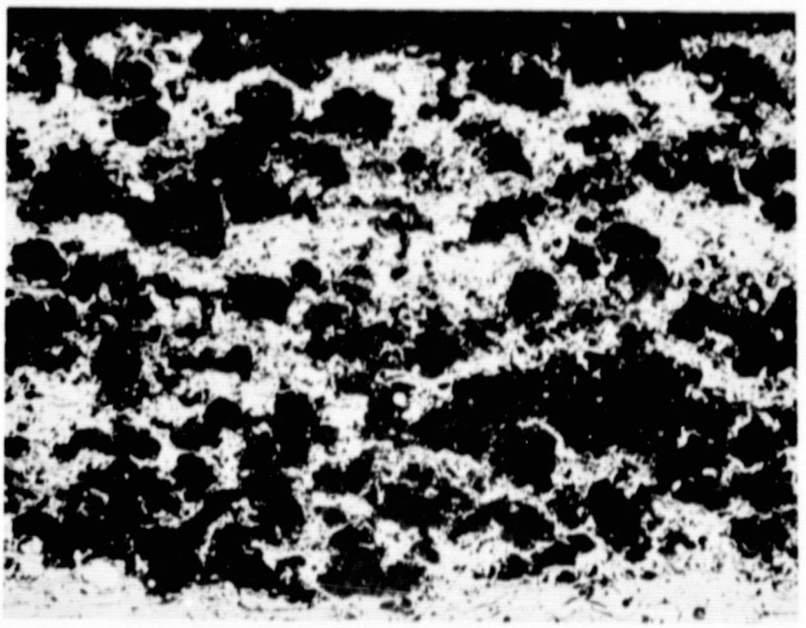

b) AlBr + 20% Ekonol

100X

Figure 25. Microstructures of (a) Cu 9Al + 20% Ekonol and (b) AlBr + 20 Ekonol showing the slightly increased density of AlBr + 20% Ekonol

TABLE 14

Particle Size Distributions for Phase III,
Task I and Task II Powders

Sieve Fraction	AlBr (Metco 51-NS)	Cu-9Al
+170	0%	7.7%
-170/+200	0%	15.6%
-200/+270	1.8%	32.0%
-270/+325	11.0%	23.7%
-325	85.3%	19.4%

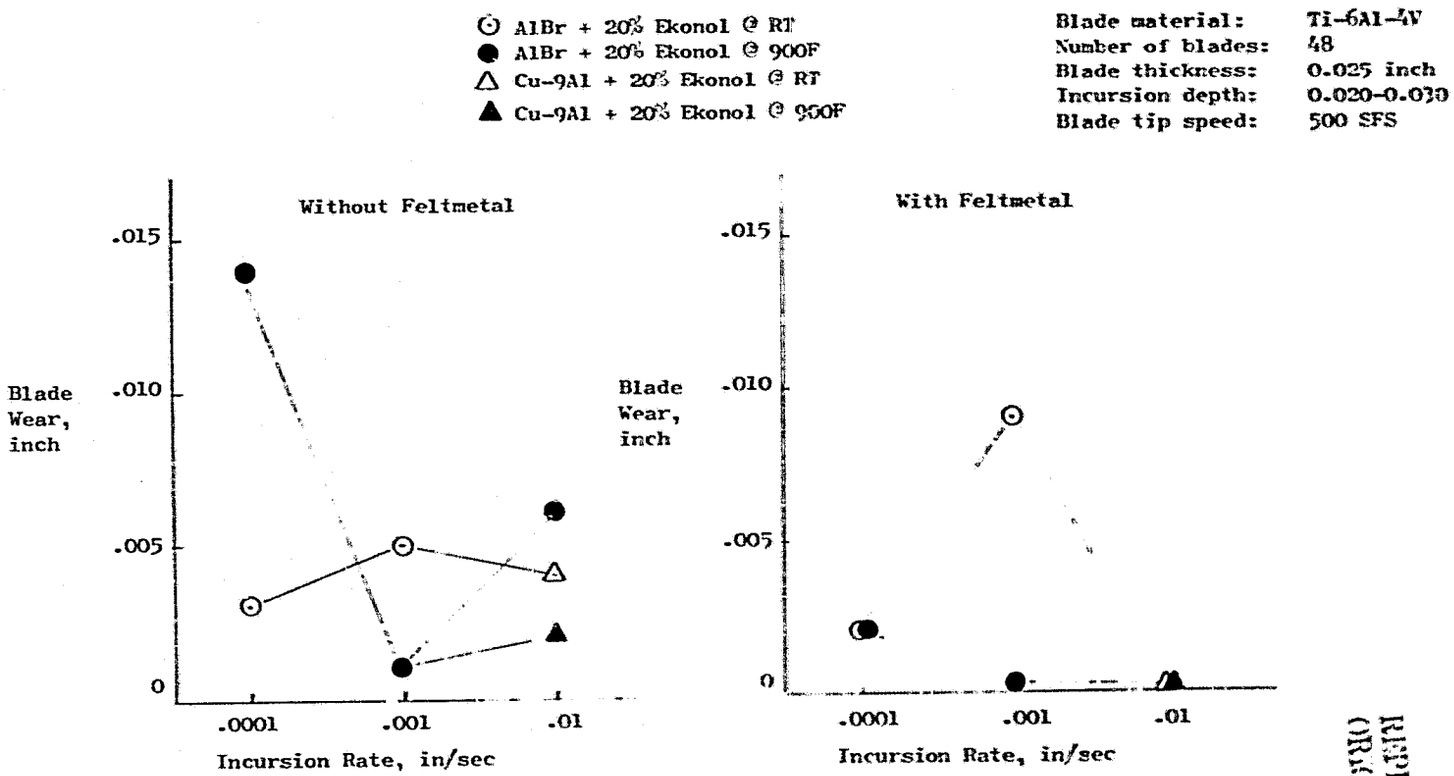

Figure 26. Blade Wear Versus Incursion Rate

and indicates that for these materials, rub performance at room temperature and 900F are significantly different. At room temperature blade wear is maximized at the .001 in/sec incursion rate whereas at 900F blade wear is minimized at the .001 in/sec rate.

Task II rub test results indicate that the point has been reached where subtle changes in spray parameters, powder size distributions and rub conditions will affect the rub performance of AlBr + 20% Ekonol coatings. This experience is consistent with prior efforts in developing abradable seal materials and indicates the need for advancing to the next development stage where the requirements for erosion resistance, thermal shock resistance, oxidation resistance, and innocuous debris must be superimposed on the abradability and smooth rub surface requirements.

5.0 CONCLUSIONS

1) Physical and mechanical properties of bulk materials help explain some of the features of the rub behavior of dense coatings but do not completely account for the differences observed in the various alloys studied.

2) Rub energy does not correlate with blade wear and cannot be used as a screening test for coating materials.

3) Al additions to Cu reduced both blade wear and scabbing.

4) An interlayer of feltmetal between the substrate and coating was found to reduce the severity of rubs (in terms of blade wear) but did not significantly affect the rub force or energy.

5) The addition of porosity to the coating produced smooth rubs but also reduced the coating's erosion resistance.

6) Significant substrate temperature rises occur only when measurable blade wear or pick-up occurred. The highest rub forces were also associated with blade wear or pick-up.

7) Subtle changes in spray parameters, powder size distributions and rub conditions were found to affect the performance and acceptability of the coatings.

   - Powder size distribution affected the density and therefore both the abradability and erosivity of the coatings.

8) In general, at low incursion rates hot rubs were more severe and at high incursion rates cold rubs were more severe.

REFERENCES

1. F.N. Rhines, Phase Diagrams in Metallurgy, McGraw-Hill (New York-London-Toronto) p. 3, 1965.

2. W.B. Pearson, A Handbook of Lattice Spacings and Structures of Metals and Alloys, Pergamon Press (New York-London-Paris-Los Angeles) 1958.

3. M. Hansen, Constitution of Binary Alloys, McGraw-Hill (New York-London-Toronto) 1958.

4. Metals Handbook, Vol. 1 (8th Ed), American Society for Metals, 1961.

5. Samuel J. Rosenberg, Nickel and Its Alloys, NBS Monograph 106, U.S. Government Printing Office (Washington) 1968.

6. Thermophysical Properties of Matter, Vol. 1, Ed. U.S. Toulonkian, R.W. Powell, C.Y. Ho, P.G. Klemens (IFI/Plenum - New York, Washin p. 1142, 1970.

7. C. Sykes and H. Evans, Proc. Roy. Soc. London, Ser A, Vol. 145, pp. 529-539 (1934).

8. W. Koster and H. Franz, Met. Rev. 6(21), 1 (1961).

9. H.J. Leamy, E.D. Gibson, and F.X. Kayser, Acta Met. 15, 1827 (1967).

10. G.E. Dieter, Jr., Mechanical Metallurgy, McGraw-Hill (New York-Toronto-London) p. 38, 1961.

11. R.W.K. Honeycombe, The Plastic Deformation of Metals, Edward Arnold Ltd. (Great Britain) pp. 6-19, 1968.

12. S.L. Case and K.R. VanHorn, Aluminum in Iron and Steel, John Wiley & Sons (New York) and Chapman & Hall (London) pp. 300-303, 1953.

13. Alloy Digest, Filing Code Ni-69, Engineering Alloy Digest, Inc. (Upper Mondain, New Jersey) 1961.

14. J.A. Williams and N. Bane, Wear 42, 341 (1977).

15. Materials Selector 77, Reinhold Publishing Co. (Stamford, Connecticut), 1976.

16. C. Sykes and J.W. Bampfylde, J. Iron & Steel Inst. 130, 389 (1934).

17. A.G. Guy, Elements of Physical Metallurgy, Allison-Wesley Publishing Co. (Reading, Mass-London) p. 428, 1960.

18. J. Weertman and J.R. Weertman, Elementary Dislocation Theory, The Macmillan Co., p. 98, 1969.

REFERENCES

(continued)

19. P.R. Thornton, T.E. Mitchell, and P.B. Hirsch, Phil Mag 7, 1349 (1962).

20. F.P. Bowden and E.H. Freitag, Proc R Soc London, Ser A, 248, 350 (1958).